28. Bowie, J. U., N. D. Clarke, C. O. Pabo, and R. T. Sauer. 1990. Identification of protein folds: matching hydrophobicity patterns of sequence sets with solvent accessibility patterns of known structures. *Proteins.* 7:257–264.

29. Ota, M., and K. Nishikawa. 1997. Assessment of pseudo-energy potentials by the best-five test: a new use of the three-dimensional profiles of proteins. *Protein Eng.* 10:339–351.

30. Sali, A., and T. L. Blundell. 1993. Comparative protein modelling by satisfaction of spatial restraints. *J. Mol. Biol.* 234:779–815.

31. Fiser, A., R. K. Do, and A. Sali. 2000. Modeling of loops in protein structures. *Protein Sci.* 9:1753–1773.

32. Baker, D., and A. Sali. 2001. Protein structure prediction and structural genomics. *Science.* 294:93–96.

33. Marti-Renom, M. A., M. S. Madhusudhan, A. Fiser, B. Rost, and A. Sali. 2002. Reliability of assessment of protein structure prediction methods. *Structure.* 10:435–440.

34. Achour, A., K. Persson, R. A. Harris, J. Sundback, C. L. Sentman, Y. Lindqvist, G. Schneider, and K. Karre. 1998. The crystal structure of H-2Dd MHC class I complexed with the HIV-1-derived peptide P18–I10 at 2.4 A resolution: implications for T cell and NK cell recognition. *Immunity.* 9:199–208.

35. Stewart, J. J. P. 1996. Application of localized molecular orbitales to the solution of semiempirical self-consistent field equations. *Int. J. Quant. Chem.* 58:133–146.

36. Sherman, D. H., P. S. Hochman, R. Dick, R. Tizard, K. L. Ramachandran, R. A. Flavell, and B. T. Huber. 1987. Molecular analysis of antigen recognition by insulin-specific T-cell hybridomas from B6 wild-type and bm12 mutant mice. *Mol. Cell. Biol.* 7:1865–1872.

37. Tan, K. N., B. M. Datlof, J. A. Gilmore, A. C. Kronman, J. H. Lee, A. M. Maxam, and A. Rao. 1988. The T cell receptor V alpha 3 gene segment is associated with reactivity to *p*-azobenzenearsonate. *Cell.* 54:247–261.

38. Bill, J., J. Yague, V. B. Appel, J. White, G. Horn, H. A. Erlich, and E. Palmer. 1989. Molecular genetic analysis of 178 I-Abm12-reactive T cells. *J. Exp. Med.* 169:115–133.

39. Cerasoli, D. M., M. P. Riley, F. F. Shih, and A. J. Caton. 1995. Genetic basis for T cell recognition of a major histocompatibility complex class II-restricted neo-self peptide. *J. Exp. Med.* 182:1327–1336.

40. Horwitz, M. S., Y. Yanagi, and M. B. Oldstone. 1994. T-cell receptors from virus-specific cytotoxic T lymphocytes recognizing a single immunodominant nine-amino-acid viral epitope show marked diversity. *J. Virol.* 68:352–357.

41. Plaksin, D., K. Polakova, P. McPhie, and D. H. Margulies. 1997. A three-domain T cell receptor is biologically active and specifically stains cell surface MHC/peptide complexes. *J. Immunol.* 158:2218–2227.

42. Bowie, J. U., R. Luthy, and D. Eisenberg. 1991. A method to identify protein sequences that fold into a known three-dimensional structure. *Science.* 253:164–170.

43. Kaye, J., and S. M. Hedrick. 1988. Analysis of specificity for antigen, Mls, and allogenic MHC by transfer of T-cell receptor alpha- and beta-chain genes. *Nature.* 336:580–583.

44. Lai, M. Z., Y. J. Jang, L. K. Chen, and M. L. Gefter. 1990. Restricted V-(D)-J junctional regions in the T cell response to lambda-repressor. Identification of residues critical for antigen recognition. *J. Immunol.* 144:4851–4856.

45. Bellio, M., Y. C. Lone, O. de la Calle-Martin, B. Malissen, J. P. Abastado, and P. Kourilsky. 1994. The V beta complementarity determining region 1 of a major histocompatibility complex (MHC) class I-restricted T cell receptor is involved in the recognition of peptide/MHC I and superantigen/MHC II complex. *J. Exp. Med.* 179: 1087–1097.

46. Lone, Y. C., M. Bellio, A. Prochnicka-Chalufour, D. M. Ojcius, N. Boissel, T. H. Ottenhoff, R. D. Klausner, J. P. Abastado, and P. Kourilsky. 1994. Role of the CDR1 region of the TCR beta chain in the binding to purified MHC-peptide complex. *Int. Immunol.* 6: 1561–1565.

47. Clark, S. P., B. Arden, D. Kabelitz, and T. W. Mak. 1995. Comparison of human and mouse T-cell receptor variable gene segment subfamilies. *Immunogenetics.* 42:531–540.

Suppression of an Already Established Tumor Growing through Activated Mucosal CTLs Induced by Oral Administration of Tumor Antigen with Cholera Toxin[1]

Ayako Wakabayashi, Yohko Nakagawa, Masumi Shimizu, Keiichi Moriya, Yasuhiro Nishiyama, and Hidemi Takahashi[2]

Priming of CTLs at mucosal sites, where various tumors are originated, seems critical for controlling tumors. In the present study, the effect of the oral administration of OVA plus adjuvant cholera toxin (CT) on the induction of Ag-specific mucosal CTLs as well as their effect on tumor regression was investigated. Although OVA-specific TCRs expressing lymphocytes requiring in vitro restimulation to gain specific cytotoxicity could be detected by OVA peptide-bearing tetramers in both freshly isolated intraepithelial lymphocytes and spleen cells when OVA was orally administered CT, those showing direct cytotoxic activity without requiring in vitro restimulation were dominantly observed in intraepithelial lymphocytes. The magnitude of such direct cytotoxicity at mucosal sites was drastically enhanced after the second oral administration of OVA with intact whole CT but not with its subcomponent, an A subunit (CTA) or a B subunit (CTB). When OVA plus CT were orally administrated to C57BL/6 mice bearing OVA-expressing syngeneic tumor cells, E.G7-OVA, in either gastric tissue or the dermis, tumor growth was significantly suppressed after the second oral treatment; however, s.c. or i.p. injection of OVA plus CT did not show any remarkable suppression. Those mucosal OVA-specific CTLs having direct cytotoxicity expressed CD8$\alpha\beta$ but not CD8$\alpha\alpha$, suggesting that they originated from thymus-educated cells. Moreover, the infiltration of such OVA-specific CD8$^+$ CTLs was observed in suppressed tumor tissues. These results indicate that the growth of ongoing tumor cells can be suppressed by activated CD8$\alpha\beta$ CTLs with tumor-specific cytotoxicity via an orally administered tumor Ag with a suitable mucosal adjuvant. ***The Journal of Immunology*****, 2008, 180: 4000–4010.**

Many malignant tumors originate from various epithelial tissues such as the skin or mucosal sites such as the esophagus, stomach, colon, or lung (1). Thus, as a cancer vaccine, it is essential to stimulate mucosal or dermal immune systems, as well as the systemic immune system, with a suitable Ag, adjuvant, and administration route as reviewed by Finn (2). Mucosal immunization using an adjuvant that enables the priming of both mucosal and systemic immunity (3, 4) may be a good way to prevent or treat mucosal tumors. In particular, the induction of mucosal CTLs that can specifically recognize tumor-derived peptide Ags presented by the corresponding class I MHC molecules seems to be one of the most important issues for eliminating tumor cells (5).

In the mucosal compartment, lymphocytes located in the intestinal epithelium are almost exclusively T cells called intraepithelial lymphocytes (IELs)[3] (3). Such IELs are mostly CD8$^+$ T cells that are classified into three distinct populations: TCR$\alpha\beta^+$CD8$\alpha\beta^+$, TCR$\alpha\beta^+$CD8$\alpha\alpha^+$, and TCR$\gamma\delta^+$CD8$\alpha\alpha^+$ (6). IELs contain cytotoxic properties and specifically eliminate virus- or parasite-infected cells (7–9); however, although spontaneous cytotoxicity of human IELs against tumor cells has been reported (10, 11), their actual specificity on tumors is still unknown. Recently, we have reported (12) that a marked increase in the number of HIV-1-specific CD8$\alpha\beta$-positive T cells among IELs was observed in HIV-1-specific TCR transgenic (Tg) mice when they received intrarectal or i.p. administration of the recombinant vaccinia virus (rVV) expressing a known restricted CTL epitope, P18 (rVV-P18), which is restricted by H-2D^d-class I MHC molecules (13). Using H-2D^d/P18 tetramers, we could detect CD8-positive, P18-specific TCR-expressing T cells in freshly isolated IELs and splenic T cells of unchallenged naive Tg mice. Although those H-2D^d/P18 tetramer-positive CD8 T cells from naive Tg mice did not show any specific cytotoxicity, freshly isolated mucosal T cells bearing CD8$\alpha\beta$ but not CD8$\alpha\alpha$ from activated Tg mice with rVV-P18 represented P18-specific cytotoxicity against tumor cells expressing the epitope, and the magnitude of cytotoxicity was much stronger than that in activated splenic T cells (12). These results suggest that in vivo activated mucosal CD8$\alpha\beta$ CTLs with tumor-specific cytotoxicity may be critical for controlling tumors expressing the specific epitope in vivo rather than systemic splenic CTLs.

Cholera toxin (CT) derived from *Vibrio cholerae* is known as a potent mucosal adjuvant comprised of one toxic A subunit (CTA) with ADP-ribosyltransferase activity and five nontoxic B subunits (CTB) responsible for binding to monosialoganglioside (GM) 1 on the cell surface (14, 15). CT adjuvant helps to produce both systemic IgG and mucosal IgA (16) as well as to induce Ag-specific

Department of Microbiology and Immunology, Nippon Medical School, Tokyo, Japan

Received for publication April 13, 2007. Accepted for publication January 7, 2008.

The costs of publication of this article were defrayed in part by the payment of page charges. This article must therefore be hereby marked *advertisement* in accordance with 18 U.S.C. Section 1734 solely to indicate this fact.

[1] This work was supported in part by Grants-in-Aid for Young Scientists from the Japan Society for the Promotion of Sciences, from the Ministry of Education, Science, Sport, and Culture, from the Ministry of Health and Labor and Welfare, Japan, and from the Promotion and Mutual Aid Corporation for Private Schools of Japan.

[2] Address correspondence and reprint requests to Dr. Hidemi Takahashi, Department of Microbiology and Immunology, Nippon Medical School, 1-1-5 Sendagi, Bunkyo-ku, Tokyo 113-8602, Japan. E-mail address: htkuhkai@nms.ac.jp

[3] Abbreviations used in this paper: IEL, intraepithelial lymphocyte; CT, cholera toxin; CTA, CT A subunit (toxic); CTB, CT B subunit (nontoxic); DC, dendritic cell; GM, monosialoganglioside; *Hp*, *Helicobacter pylori*; LPL, lamina propria lymphocyte; MadCAM-1, mucosal addressin cell-adhesion molecule-1; OVA-CT, CT-conjugated OVA; PP, Peyer's patch; rVV, recombinant vaccinia virus; SC, spleen cell; Tg, transgenic; TIL, tumor-infiltrating lymphocyte.

 0022-1767/08/$2.00

$CD4^+$ T cell responses in the spleen, reflecting the systemic compartment, and in Peyer's patches (PPs), reflecting the mucosal compartment (17). In addition, it has been demonstrated (18) that OVA-specific CTLs could be primed in C57BL/6 mice following oral exposure to a combination of OVA with CT, and specific cytotoxic activity was detected from spleen cells (SCs) only when they were restimulated in vitro with irradiated OVA-expressing syngeneic tumor cells, E.G7-OVA, which are OVA gene-transfected EL4 thymoma cells (19, 20). Also, intranasal preimmunization with OVA peptide (SIINFEKL) plus CT primed similar OVA-specific CTLs in the spleen of C57BL/6 mice, and the immunized mice were protected from the development of transferred E.G7-OVA (21).

Moreover, it has been shown that adoptive transfer of naive $CD8^+$ OVA-specific OT-I T cells into E.G7-OVA tumor-bearing syngeneic mice did not inhibit tumor growth, although adoptive transfer of preactivated OT-I CTL in vitro inhibited tumor growth in a dose-dependent manner (22). Furthermore, it has recently been reported that vaccination with dendritic cells (DCs) prepulsed ex vivo with CT-conjugated OVA (OVA-CT) gave rise to OVA-specific splenic $CD8^+$ T cells that produced IFN-γ, were cytotoxic to E.G7-OVA cells in vivo, and rejected already established in vivo E.G7-OVA tumors associated with high numbers of tumor-infiltrating $CD8^+$ T cells (23), indicating that the elimination of previously established tumor cells might require the infiltration of tumor-specific activated $CD8^+$ CTLs.

In the present study, we found two distinct types of $CD8\alpha\beta$-positive T cells among freshly isolated lymphocytes expressing OVA-specific TCRs, which can be detected by OVA peptide-bearing tetramers. One is in an activated effector state with cytotoxic activity and the other is a resting state and may gain cytotoxicity when stimulated with an OVA epitope peptide in vitro. Based on the observations, we defined direct cytotoxicity as the former state, in which freshly isolated and unstimulated CD8 T cells had specific cytotoxicity. Therefore, by comparing systemic SCs, we asked whether OVA-specific cytotoxic activity could be observed among freshly isolated IELs in mice orally administered OVA plus CT and examined whether those activated CTLs would reject or suppress the growth of already established tumors. Consequently, we observed dominant $TCR\alpha\beta$ and $CD8\alpha\beta$ OVA-specific CTL activities in freshly isolated IELs rather than in SCs after the oral administration of OVA plus CT, and such mucosal CTL activities could be expanded after oral boosting. Moreover, the growth of E.G7-OVA inoculated into the stomach or the epidermis was significantly suppressed, accompanied by the expansion of activated mucosal CTLs, and the infiltration of such OVA-specific $CD8\alpha\beta^+$ CTLs was observed in suppressed dermal tumor tissues. These results indicate that the growth of ongoing tumor cells can be suppressed in vivo by activated $CD8\alpha\beta$ CTLs with tumor-specific cytotoxicity via an orally administered tumor Ag with a suitable mucosal adjuvant.

Materials and Methods

Mice

Six- to 8-wk-old female C57BL/6 ($H\text{-}2^b$) mice were purchased from Charles River Japan, maintained in microisolator cages under pathogen-free conditions, and fed autoclaved laboratory chow and water. All animal experiments were performed according to guidelines for the care and use of laboratory animals set by the National Institutes of Health (NIH; Bethesda, MD) and approved by the Review Board of Nippon Medical School (Tokyo, Japan).

Oral and systemic immunization

Chicken egg OVA, grade V (Sigma Aldrich), was dissolved in sterilized PBS. Mice were orally administered 100 mg of OVA or 10 μg of CT (List Biological Laboratories) alone or 100 mg of OVA plus 10 μg of CT, CTA, or CTB (List Biological Laboratories) in 0.3 ml of PBS. In some experiments, mice were orally administered 10 mg of OVA plus 10 μg of CT. For systemic immunization, mice were i.p. or s.c. injected with 100 mg of OVA or the same dose of OVA plus 10 μg of CT.

Preparation of IELs, lamina propria lymphocytes (LPLs), SCs, and tumor-infiltrating lymphocytes (TILs)

IELs were prepared by the method described previously (12). In brief, after the small intestine, large intestine, or stomach was obtained from mice, fecal materials were flushed from the lumen with HBSS (Invitrogen Life Technologies) and connective tissues were carefully removed. The obtained guts were inverted and cut into several segments that were transferred to a 50-ml conical tube (Becton Dickinson Labware) containing 45 ml of HBSS with 5% FCS, 100 U/ml penicillin (Invitrogen Life Technologies), and 100 μg/ml streptomycin (Invitrogen Life Technologies). The tube was then shaken at 37°C for 45 min (horizontal position; orbital shaker at 150 rpm). Harvested cells from the intestinal epithelium were passed through a 10-ml syringe column containing loosely packed glass wool to remove tissue debris. Subsequently, the cells were suspended in 30% Percoll solution (Amersham Biosciences) and centrifuged for 20 min at 1,800 rpm. Cells at the bottom of the solution were then subjected to Percoll discontinuous gradient centrifugation for 20 min at 1,800 rpm and IELs were recovered at the interphase of 44 and 70% Percoll solutions. LPLs were prepared by the method described previously (24). In brief, after the small intestine, large intestine, or stomach was dissected from mice, fecal material was flushed from the lumen with HBSS and PPs were carefully removed. The obtained guts were inverted and cut into several segments that were transferred to a 50-ml conical tube containing 45 ml of HBSS with 5% FCS and 1 mM EDTA (Wako Pure Chemical Industries). The tube was shaken at 37°C for 45 min (horizontal position; orbital shaker at 150 rpm). The gut segments were then washed with PBS and shaken in 40 ml of HBSS with 5% FCS and 0.1 mg/ml collagenase (Sigma-Aldrich) at 37°C for 45 min (horizontal position; orbital shaker at 60 rpm). Harvested cells were passed through a nylon mesh and suspended in 40% Percoll solution, and then 70% Percoll solution was underlain. The solution was centrifuged for 20 min at 1,800 rpm and LPLs were recovered at the interphase of 40 and 70% Percoll solutions. These procedures provided >95% viable lymphocytes with a cell yield of $5\text{–}10 \times 10^6$ of small intestinal IELs, $2\text{–}3 \times 10^5$ of large intestinal IELs, $7\text{–}12 \times 10^3$ of gastric IELs, $4\text{–}9 \times 10^5$ of small intestinal LPLs, $1\text{–}3 \times 10^5$ of large intestinal LPLs, or $5\text{–}9 \times 10^4$ of gastric LPLs per mouse. The cells were suspended in complete T cell medium (25) composed of RPMI 1640 medium (Sigma-Aldrich) supplemented with 2 mM L-glutamine (ICN Biomedicals), 1 mM sodium pyruvate (Invitrogen Life Technologies), 0.1 mM nonessential amino acid (Invitrogen Life Technologies), a mixture of vitamins (ICN Biomedicals), 1 mM HEPES (Invitrogen Life Technologies), 100 U/ml penicillin (Invitrogen Life Technologies), 100 μg/ml streptomycin (Invitrogen Life Technologies), 50 μM 2-ME (Sigma-Aldrich), and heat-inactivated 10% FCS. For TIL preparation, tumors were removed from mice, incubated in 1 mg/ml collagenase (Wako Pure Chemical Industries) with PBS at 37°C for 1 h, and crushed gently. TILs were prepared using Percoll solutions as described in the previous paragraph regarding IEL preparation. The spleen was aseptically removed and a single cell suspension was prepared. For osmotic hemolysis, single cells were suspended in 0.1× PBS and an equal amount of 2× PBS was added immediately. To enrich IELs, LPLs, and TILs from mice, the interface between the 40 and 70% Percoll solutions (26), in which NK cells and unfractionated SCs, which may also include NK cells, must be included, was collected.

Flow cytometry analysis

Cells were double-stained with PE-labeled $H\text{-}2K^b$/OVA tetramer-SIINFEKL (Beckman Coulter) or $H\text{-}2K^b$/PB1 tetramer-SSYRRPVGI (Medical & Biological Laboratories) and FITC-labeled anti-mouse TCRβ, CD8α (BD Pharmingen), or CD8β (Caltag Laboratories). Peptide PB1 703–711, SSYRRPVGI, for the control tetramer was derived from influenza virus (27). Dead cells were determined using 7-aminoactinomycin D viability dye (Beckman Coulter) and stained cells were analyzed by FACScan using the CellQuest program (BD Biosciences).

In vitro restimulation of SCs or IELs with E.G7-OVA

Lymphocytes were restimulated in vitro by the method described previously (19). Freshly isolated SCs (3×10^7) or IELs (3×10^7) were restimulated with 3×10^6 irradiated (20,000 rad) E.G7-OVA cells (19, 20) ($H\text{-}2^b$; American Type Culture Collection) in 10 ml of complete T cell medium per upright 25-cm^2 flask in 5% CO_2 at 37°C for 6 days. Six days later, the viability of the lymphocytes was 35–51% in SCs and 16–26% in IELs. The

in vitro restimulated cells were collected and their OVA-specific cytotoxicity was measured by the following procedure.

CTL assay

For the CTL assay, freshly isolated IELs, SCs, or TILs were used. Cytolytic activity was measured using a standard ^{51}Cr-release assay as previously described (12). In brief, various numbers of effector cells were incubated with 3×10^3 ^{51}Cr-labeled targets for 6 h at 37°C in 200 μl of RPMI 1640 medium containing 10% FCS in round-bottom 96-well cell culture plates (BD Biosciences). After incubation, the plates were centrifuged for 10 min at $330 \times g$, and 100 μl of cell-free supernatants were collected to measure radioactivity with a Packard Auto-Gamma 5650 counter (Hewlett-Packard Japan). Maximum release was determined from the supernatant of cells that had been lysed by the addition of 5% Triton X-100, and spontaneous release was determined from target cells incubated without added effector cells. The percentage of specific lysis was calculated as 100 × (experimental release − spontaneous release)/(maximum release − spontaneous release). SEs of the means of triplicate cultures were always <5% of the mean. Each experiment was performed at least three times.

Measurement of in vivo antitumor effects

E.G7-OVA cells (5×10^6), OVA gene-transfected EL4 thymoma cells (19, 20), were implanted into the gastric or dermal tissue of syngeneic C57BL/6 mice (H-2^b). For tumor implantation into the gastric tissue, mice were anesthetized and underwent an abdominal operation and then E.G7-OVA cells in 50 μl of RPMI 1640 were injected into the muscle layer of the stomach using a syringe with a 29-gauge needle (Terumo). For implantation into the dermal tissue, mice were anesthetized and E.G7-OVA cells in 100 μl of RPMI 1640 were injected intradermally by a 29-gauge needle syringe. On day 3 after implantation into the gastric or dermal tissue, when the tumor mass became visible, tumor-bearing mice were orally or systemically administered OVA plus CT as described above. Seven days after the first administration, some of the mice were similarly boosted with the same materials. The growing tumors implanted into the gastric or dermal tissues were followed by measuring the length (a) and width (b), the and tumor volume (V) was calculated according to the formula $V = ab^2/2$ as reported previously (28). When the longer axis of each tumor was >20 mm, all mice were anesthetized and sacrificed according to the guidelines for the care and use of laboratory animals set by the NIH.

Histological analysis of tumor tissues

Freshly excised tumor tissues were embedded in Tissue-Tek OCT compound (Sakura Finetek) at −80°C. Tissue segments were sectioned at 6 μm using a cryostat. Sections were placed on a poly-L-lysine-coated glass slide, air dried, and then fixed in 10% formalin PBS for 5 min and stained with H&E. For immunohistochemical staining, sections were fixed in cold acetone for 5 min and incubated with blocking solution (Block-ace; Dainippon Pharmaceutical) for 30 min at 37°C and then incubated with biotin-conjugated rat anti-CD8β Ab (Caltag Laboratories) or control isotype-matched rat IgG2a Ab (Caltag Laboratories) overnight at 4°C. Endogenous peroxidase was quenched by incubation in 0.3% H_2O_2 and 0.1% NaN_3 in distilled water for 10 min. The sections were incubated with avidin-biotin peroxide complexes (Vectastain ABC kit; Vector Laboratories) followed by color reaction with a Vectastain diaminobenzidine substrate kit (Vector Laboratories).

Statistical analysis

Student's t test was used to determine the statistical significance of differences between groups in tumor growth. Data were considered significant at $p < 0.05$.

Results

Priming of OVA-specific CD8αβ-positive CTLs with direct cytotoxicity via oral administration with OVA plus CT

It has been reported that OVA-specific CTLs could be primed in C57BL/6 mice by oral or i.v. immunization with OVA plus CT together with nontoxic CTB, and specific cytotoxic activity was detected from immune SCs only when they were restimulated in vitro with irradiated OVA-expressing syngeneic tumor (E.G7-OVA) cells (18). It has also been shown that activated CTLs but not naive primed CTLs could represent antitumor responses in vivo (22). Similarly, we have recently observed in HIV-1-specific CTL-TCR transgenic mice that activated CTLs but not freshly isolated TCR-bearing CD8αβ-positive T cells showed specific cytotoxicity, and the most critical sites for activating TCR-bearing CD8αβ T cells were mucosal compartments when Tg mice were administered a specific Ag for TCR (12).

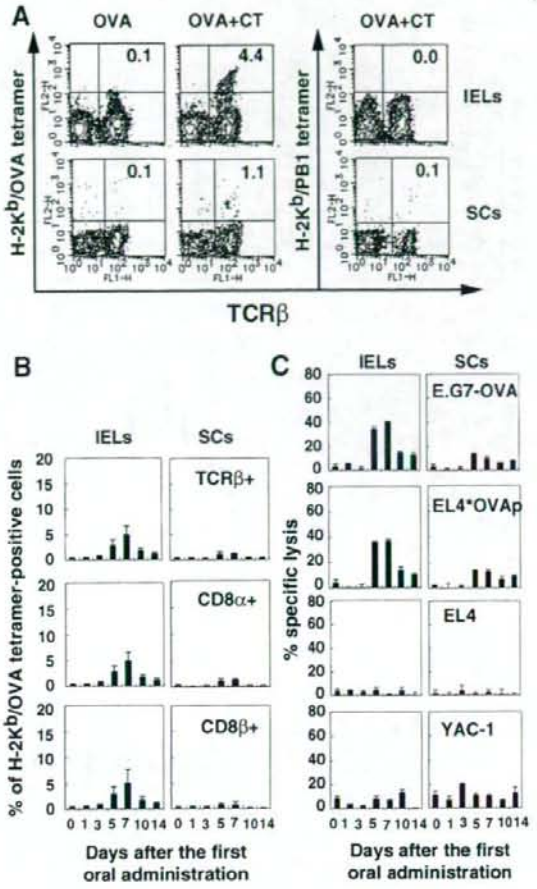

FIGURE 1. Analysis of OVA-specific direct cytotoxicities in IELs and SCs after primary immunization with OVA plus CT. *A*, Analysis of H-2K^b/OVA tetramer-positive cells. C57BL/6 mice were orally administered OVA or OVA plus CT once. IELs and SCs were collected from mice 5 days after the first oral administration, stained with either PE-labeled H-2K^b/OVA tetramer-SIINFEKL or H-2K^b/PB1 tetramer-SSYRRPVGI together with FITC-labeled anti-mouse TCRβ, and analyzed by flow cytometry. Each value represents the percentage of cells expressing both indicated markers. Data are representative of three independent experiments. *B*, Kinetics of H-2K^b/OVA tetramer-positive cells after primary immunization. C57BL/6 mice were orally administered OVA plus CT once. IELs and SCs were collected from mice at various days after the first oral administration, stained with PE-labeled H-2K^b/OVA tetramer together with FITC-labeled anti-mouse TCRβ, CD8α, or CD8β, and analyzed by flow cytometry. The results are shown as the mean ± SD of four mice. *C*, Kinetics of OVA-specific direct cytotoxic responses. C57BL/6 mice were orally primed and cells were collected as described in *B*. OVA-specific CTL responses were measured by ^{51}Cr-release assay using E.G7-OVA cells (H-2^b), YAC-1 cells, and EL4 cells (H-2^b) pulsed with or without 4 μM OVA-peptide, SIINFEKL, as target cells. E:T ratio was 100:1. The results shown as the mean ± SD in triplicate of pooled cells from two mice are representative of three independent experiments.

These findings prompted us to examine whether direct OVA-specific cytotoxic activity could be induced among IELs in mice

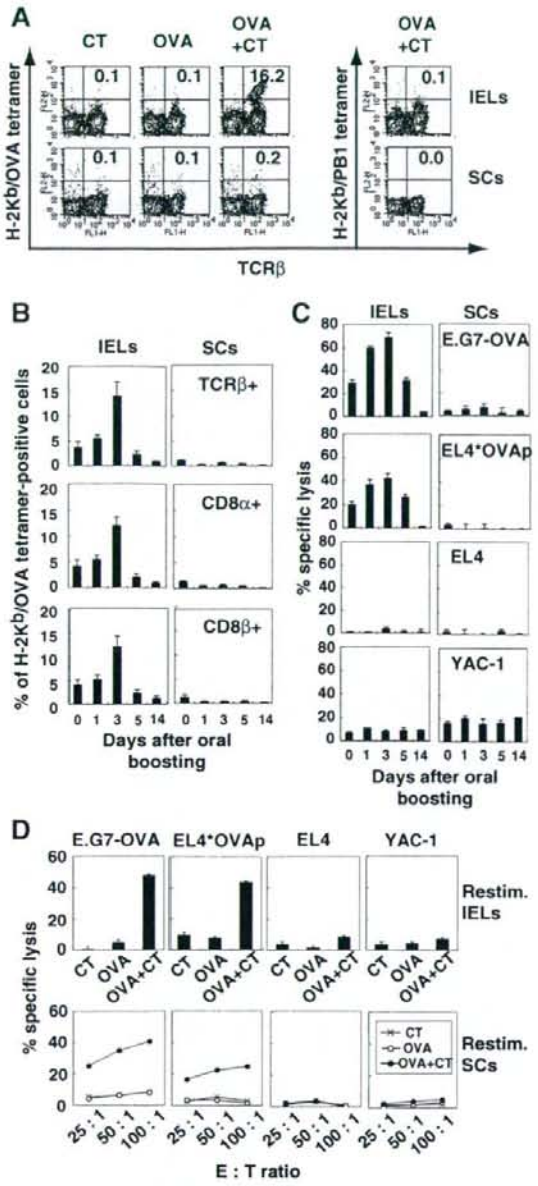

FIGURE 2. Expansion of direct OVA-specific cytotoxicities after oral boosting with OVA plus CT. *A*, Activated H-2K^b/OVA tetramer-positive cells after oral boosting. C57BL/6 mice were orally administered CT, OVA, or OVA plus CT once weekly for 2 wk. IELs and SCs were collected from mice 3 days after the second oral boost and stained with PE-labeled H-2K^b/OVA tetramer or H-2K^b/PB1 tetramer together with FITC-labeled anti-mouse TCRβ. Each value represents the percentage of cells expressing both indicated markers. Data are representative of three independent experiments. *B*, Kinetics of H-2K^b/OVA tetramer-positive cells after oral boosting. C57BL/6 mice were orally administered OVA plus CT once weekly for 2 wk. IELs and SCs were collected from mice at various days after the second oral boost, stained with PE-labeled H-2K^b/OVA tetramer together with FITC-labeled anti-mouse TCRβ, CD8α, or CD8β, and analyzed by flow cytometry. The results are shown as the mean ± SD of four mice. *C*, Kinetics of the secondary expansion of OVA-specific direct CTL responses. C57BL/6 mice were treated orally and the cells were collected as described in *B*. OVA-specific CTL responses were measured by ^{51}Cr-release assay using E.G7-OVA cells, YAC-1 cells, and EL4 cells pulsed with or without OVA peptide as targets. The E:T ratio is 100:1. The results shown as the mean ± SD in triplicate of pooled cells from two mice are representative of three independent experiments. *D*, Activation of OVA-specific CTLs by in vitro restimulation (Restim.). C57BL/6 mice were orally administered CT, OVA, or OVA plus CT once weekly for 2 wk. IELs (3×10^7) and SCs (3×10^7) were collected from mice 9 days after the second oral boost, and cocultured with 3×10^6 irradiated E.G7-OVA. Six days later, OVA-specific lysis of stimulated IELs and SCs was measured by ^{51}Cr-release assay. The E:T ratio is 100:1 in IELs and 100:1, 50:1, or 25:1 in SCs. The results are shown as the mean ± SD in IELs or the mean in SCs in triplicate of pooled cells from two mice. Data are representative of three independent experiments.

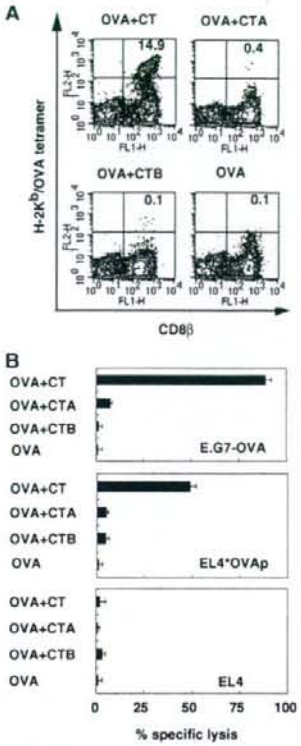

FIGURE 3. Both subunits, CTA and CTB, are essential for the induction of OVA-specific CTLs. C57BL/6 mice were orally administered OVA or OVA plus intact CT, CTA subunit or CTB subunit once weekly for 2 wk. IELs were collected from mice 3 days after the second oral administration. *A*, IELs were stained with PE-labeled H-2K^b/OVA tetramer and FITC-labeled anti-mouse CD8β. Each value represents the percentage of cells expressing both indicated markers. *B*, OVA-specific CTL responses of isolated IELs were measured by ^{51}Cr-release assay using E.G7-OVA cells, EL4 cells pulsed with or without OVA peptide as targets. The E:T ratio is 100:1. Data are shown as the mean ± SD in triplicate of pooled cells from two mice. The results are representative of three independent experiments for both *A* and *B*.

administered OVA plus CT orally without requiring in vitro restimulation. To carry out this experiment, we used a H-2K^b/OVA tetramer to detect cells expressing OVA-specific TCR in freshly isolated IELs as well as in the SCs of primed mice 5 days after immunization. Also, to evaluate the purity of IELs, CD103 (integrin

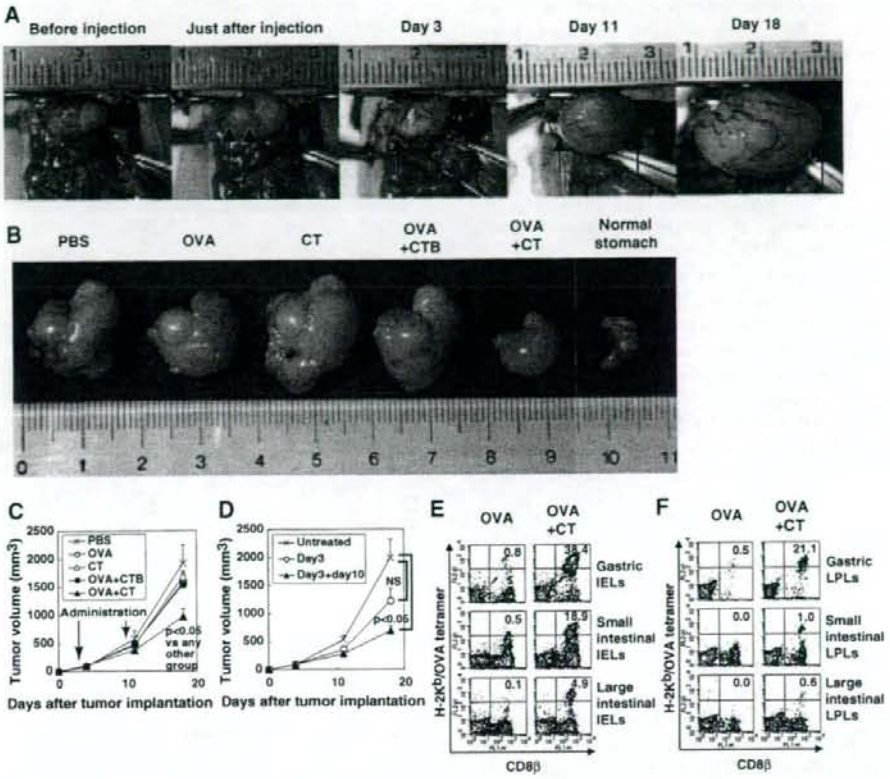

FIGURE 4. Suppression of the growth of a tumor implanted into gastric tissue by oral administration of OVA plus CT. *A*, Growth of visible tumor after implantation of E.G7-OVA cells into gastric tissue. C57BL/6 mice were implanted with 5×10^6 E.G7-OVA cells into the muscle layer of the stomach. Each day, the same mice were anesthetized and underwent an abdominal operation, and tumors were observed. Arrows point to both ends of the longer axis in the tumor. *B*, C57BL/6 mice were implanted with 5×10^6 E.G7-OVA cells into the muscle layer of the stomach. Three days later, tumor-bearing mice were orally administered PBS, OVA, CT, OVA plus CTB subunit, or OVA plus CT. Seven days later, the second oral administration was performed in the same manner. Stomachs were excised from the mice 18 days after tumor implantation, as well as from untreated, normal mice. *C*, Tumor volumes were calculated based on the formula described in *Materials and Methods*, and the results are shown as the mean ± SEM. The results were obtained from 9–13 mice per group. $p < 0.05$ indicates statistically significant difference between OVA plus CT (▲) and any other groups. *D*, C57BL/6 mice were implanted with E.G7-OVA cells in the stomach. Three days later, tumor-bearing mice were orally administered OVA plus CT or left untreated. Seven days later, some orally immunized mice were boosted in the same manner or left untreated. The results are shown as the mean ± SEM of 5–7 mice per group. $p < 0.05$ and NS indicate statistically significant and not significant differences, respectively, between the boosted (▲) and nonboosted (○) groups and the untreated group (×). *E* and *F*, Induction of CD8β and H-2K^b/OVA tetramer-positive cells in IELs (*E*) and LPLs (*F*) of the stomach, small intestine, or large intestine after oral administration of OVA plus CT. C57BL/6 mice were orally administered OVA or OVA plus CT once weekly for 2 wk. IELs and LPLs were collected from mice 3 days after the second oral administration. Cells were stained with PE-labeled H-2K^b/OVA tetramer and FITC-labeled anti-mouse CD8β. Each value represents the percentage of cells expressing both indicated markers. The results are representative of three independent experiments.

α-IEL chain)-positive cells in the collected samples were examined by flow cytometry. CD103 is highly expressed on >90% of IELs (29, 30) but on only 15% of SCs (31). In the present study, CD103-positive cells occupied >90% of IELs and ~15% of SCs (data not shown). Although a small number of OVA-specific TCR-expressing cells were detected in both IELs (4.5–5.0%) and SCs (1.0–1.5%) after oral administration of OVA plus CT in comparison with control H-2K^b/PB1-positive cells, H-2K^b/OVA tetramer-positive cells were not observed in mice treated with OVA alone (Fig. 1*A*). Such OVA peptide-specific TCR-expressing cells were TCRγδ negative (data not shown) and both CD8α and β positive (Fig. 1*B*). The number of tetramer-positive cells, to which the magnitude of direct OVA-specific cytotoxicity closely corresponded, was maximal at day 7 after oral immunization with both IELs and SCs (Fig. 1*B*), but it did not correspond to NK cell activity as measured against YAC-1 targets (Fig. 1*C*). The results clearly demonstrate that direct OVA-specific CTL cytotoxicity is dominantly observed in mucosal IELs after primary oral administration of OVA plus CT.

Augmentation and kinetics of direct OVA-specific cytotoxicity by CD8αβ CTLs among IELs and SCs via oral boosting with OVA plus CT at day 7 after the primary administration

As shown above, because only 4.5–5.0% of IELs were temporarily activated by a one-shot oral administration, we extensively examined the effect of oral boosting with OVA plus CT at various days after primary immunization. The number of H-2K^b/OVA tetramer-positive cells was significantly enhanced among IELs but not among SCs when primed mice were boosted (Fig. 2*A*). Such an effect was highest when mice were boosted at day 7 after initial

priming (data not shown). Tetramer-positive cells were again TCRβ-, CD8α-, and CD8β-positive IELs and their number peaked at day 3 after boosting (Fig. 2*B*). Correspondingly, direct OVA-specific cytotoxicity was greatly enhanced among IELs and the maximal cytotoxicity of IELs was observed at day 3 after boosting (Fig. 2*C*), although such direct cytotoxicity appeared to be completely lost in SCs (Fig. 2*C*). Nonetheless, SCs showed good epitope-specific cytotoxicity similar to that of IELs when they were restimulated in vitro with irradiated E.G7-OVA (Fig. 2*D*), suggesting that the priming effect by the oral administration of OVA plus CT also remained in systemic SCs.

It should be noted that the memory of OVA-specific CTLs persisted among IELs but not SCs. When secondary boosting with OVA plus CT was performed even 6 mo after primary boosting at day 7, the number of H-2K^b/OVA tetramer-positive cells was still detected at ~6% in IELs, and they showed remarkable direct cytotoxicity of ~84.5% against E.G7-OVA cells and 58.4% against EL4 cells pulsed with OVA peptide 3 days after secondary boosting (data not shown). Again, we could not detect any measurable direct cytotoxicity in the SCs of secondary boosted mice (data not shown).

Both CTA and CTB subunits are required to induce direct OVA-specific cytotoxicity in IELs

CT is comprised of a single A subunit, CTA, and five B subunits, CTB. When OVA was administered orally to mice with either 10 μg of CTA or an equal amount of CTB, H-2K^b/OVA tetramer-positive cells as well as direct OVA-specific cytotoxicity could not be detected in IELs (Fig. 3, *A* and *B*) and SCs (data not shown), although a significant number of tetramer-positive cells and strong direct OVA-specific cytotoxicity were observed among IELs of mice administered orally with OVA plus 10 μg of intact CT (Fig. 3, *A* and *B*). Even when using 50 μg of CTA or CTB for the administration of OVA, direct cytotoxicity was not observed (data not shown); therefore, both CTA and CTB subunits are required to induce direct Ag-specific cytotoxicity.

Effects of oral administration and booting with OVA plus CT on OVA-expressing tumor growth established in the stomach

We then examined in vivo antitumor effects of oral administration with tumor Ag plus CT on already established tumors growing in mice. C57BL/6 mice were implanted with 5×10^6 syngeneic E.G7-OVA cells into the muscle layer of the stomach (Fig. 4*A*). Three days later, tumor-bearing mice (Fig. 4*A*) were orally administered various combinations of OVA plus adjuvant and boosted with the same materials 7 days after the initial oral administration. To our surprise, tumor growth in the stomach of mice orally administered OVA plus CT twice was visually (Fig. 4*B*) and significantly ($p < 0.05$; Fig. 4*C*) suppressed on day 18 after tumor implantation as compared with other control groups such as OVA plus CTB or CT alone. However, when tumor-bearing mice were orally administered OVA plus CT once and without boosting, no statistically significant suppression was observed on day 18 as compared with untreated control mice, although a slight suppressive effect could be seen (Fig. 4*D*). Therefore, two oral administrations of tumor-Ag plus CT with an appropriate interval induced significant ongoing tumor suppression.

As previously shown, direct OVA-specific cytotoxicity among small intestinal IELs was greatly enhanced after boosting with OVA plus CT (Fig. 2, *A*, *B*, and *C*). We also examined whether direct OVA-specific CTLs were induced in the IELs and LPLs of the stomach, small intestine, and large intestine from boosted mice in which gastric tumor growth was significantly suppressed. We observed an increase in the number of H-2K^b/OVA tetramer-positive

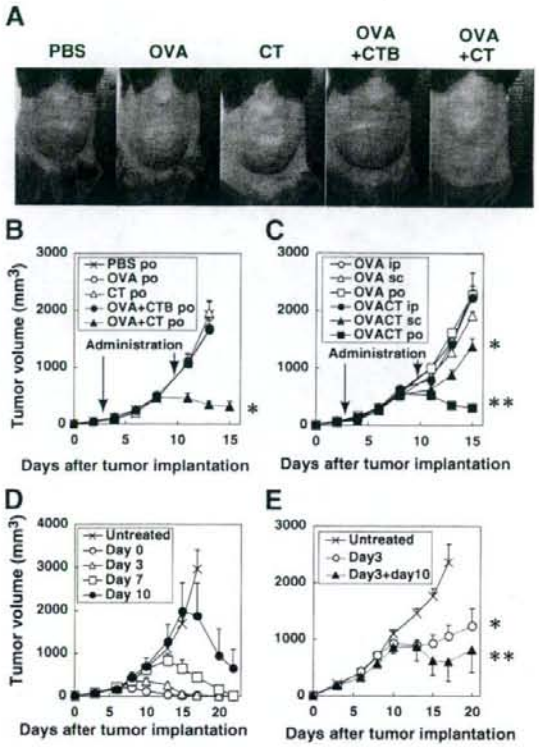

FIGURE 5. Suppression of intradermal tumor growth by oral administration with OVA plus CT. C57BL/6 mice were implanted intradermally with 5×10^6 E.G7-OVA cells. Three days later, tumor-bearing mice were orally administered PBS, OVA, CT, OVA plus CTB subunit, or OVA plus CT. Seven days later, the second oral administration was performed in the same manner. *A*, Visual suppressive effect of oral inoculation of OVA plus CT on dermal tumor growth. *B*, Tumor volumes were calculated based on the formula described in *Materials and Methods* and the results are shown as the mean ± SEM. Results were obtained from 5–6 mice per group. The asterisk (*) indicates statistically significant difference between the OVA plus CT group (closed triangle) and any other group at 11 days ($p < 0.05$) and 13 days ($p < 0.005$) after tumor inoculation. *C*, C57BL/6 mice were implanted intradermally with E.G7-OVA cells. Three days later, tumor-bearing mice were intraperitoneally (ip), subcutaneously (sc), or orally (po) administered OVA alone or OVA plus CT. Seven days later, the second treatment was performed in the same manner. The results are shown as the mean of tumor volumes ± SEM. Results were obtained from 5–6 mice per group. The asterisk (*) shows statistically significant differences ($p < 0.05$) between the s.c. OVA plus CT group (▲) and the s.c. OVA alone group at days 11, 13, and 15 after tumor implantation, and the two asterisks (**) indicate significant differences ($p < 0.01$) between the oral OVA plus CT group (■) and the oral OVA alone group on the same days. *D*, C57BL/6 mice were implanted intradermally with E.G7-OVA cells. The mice were orally administered once with OVA plus CT at day 0, 3, 7, or 10 after tumor implantation. The results are shown as the mean of tumor volumes ± SEM. Results were obtained from 10–12 mice per group. In single orally administered groups, significant tumor regression ($p < 0.05$) was observed at 7 days after oral administration compared with the untreated group. *E*, C57BL/6 mice were implanted intradermally with E.G7-OVA cells. Three days later, tumor-bearing mice were orally administered a low dose (10 mg) of OVA plus CT. Seven days later, some orally administered mice were boosted in the same manner. The results obtained from 5- mice per group are shown as the mean of tumor volumes ± SEM. The asterisk (*) indicates statistically significant differences ($p < 0.01$) between the nonboosted (○) and untreated mice (×) groups at days 15 and 17 after tumor implantation, and the two asterisks (**) indicate significant differences ($p < 0.005$) between the boosted (▲) and untreated groups on the same days.

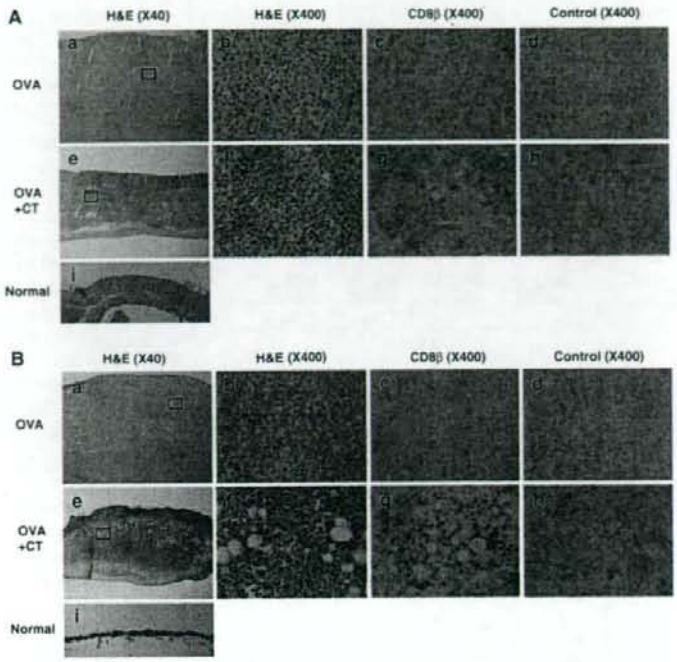

FIGURE 6. Infiltration of CD8$\alpha\beta$ positive lymphocytes into tumor tissues in mice orally administered OVA plus CT. C57BL/6 mice were implanted with 5×10^6 E.G7-OVA cells into the muscle layer of the stomach (*A*, *a–h*) or skin (*B*, *a–h*). Three days later, tumor-bearing mice were orally administered OVA (*A*, *a–d*, and *B*, *a–d*) or OVA plus CT (*A*, *e–h* and *B*, *e–h*). Seven days later, the second oral administration was performed in the same manner. Gastric and dermal tumor tissues were removed from mice 3 days after the second oral boost. Frozen sections of tumor tissues and normal tissues were prepared and stained with H&E (*A*, *a*, *b*, *e*, *f*, and *i* and *B*, *a*, *b*, *e*, *f*, and *i*) or immunohistochemically stained with biotin-conjugated rat anti-CD8β mAb (*A*, *c* and *g*, and *B*, *c* and *g*) or control isotype-matched rat IgG2a Ab (*A*, *d* and *h*, and *B*, *d* and *h*). Image magnification is either ×40 (*A*, *a*, *e*, and *i* and *B*, *a*, *e*, and *i*) or ×400 (*A*, *b–d* and *f–h* and *B*, *b–d* and *f–h*). *A*, *b* and *f* and *B*, *b* and *f* are enlarged images (×400) of the squared areas in the images (×40) of *A*, *a* and *e* and *B*, *a* and *e*, respectively.

cells among IELs in the stomach (38.4%) as well as the small (18.9%) and large intestine (4.9%) of tumor-suppressed mice (Fig. 4*E*) and also among LPLs in the stomach (21.1%) as well as the small (1.0%) and large (0.6%) intestine (Fig. 4*F*). Thus, the ability of LPLs to suppress tumor growth may be weaker than that of IELs. The results suggest that oral administration of Ag plus intact CT with appropriate mucosal boosting apparently suppressed the already established tumor growth in gastric tissue, particularly after oral boosting, probably through the activation of Ag-specific CTLs in the mucosal compartment.

Effects of oral administration and boosting with OVA plus CT on already established OVA-expressing dermal tumor growth

Next, we investigated the effect of the oral administration of tumor Ag plus CT on tumor growth in the skin, where the digestive tract is not directly associated. Mice were implanted with 5×10^6 E.G7-OVA cells intradermally. Three days later, tumor-bearing mice were orally administered various combinations of OVA plus adjuvant and boosted with the same materials 7 days after the initial oral administration. Interestingly, intradermal tumor growth was again strongly suppressed visually 11 days after tumor implantation in the dermis of mice orally administered OVA plus CT as compared with various other groups (Fig. 5*A*). This visual effect was confirmed by calculating the volume of the tumors established at day 11 and day 13 in each group ($p < 0.05$ and $p < 0.005$, respectively; Fig. 5*B*). We also examined the effect of the administration of tumor Ag plus CT via various routes on intradermal tumor growth. Although a slight suppression was observed by s.c. inoculation of OVA plus CT, tumor growth was not suppressed at all by i.p. administration in comparison with the oral treatment group (Fig. 5*C*). It should be noted that tumor growth in the dermis was markedly suppressed even by a single oral administration of OVA plus CT on day 0, 3, 7, or 10 after tumor implantation (Fig. 5*D*). In each group, tumor growth was suppressed ($p < 0.05$) and the tumor volume was small around 7 days after oral administration. Unexpectedly, there was almost no difference in the suppressive effects on tumor growth between mice treated with a single administration and boosted mice showing much stronger direct cytotoxicity (data not shown). However, when the dosage quantity of OVA was decreased by one-tenth, tumor growth in boosted mice was more significantly ($p < 0.005$) suppressed than in nonboosted mice ($p < 0.01$; Fig. 5*E*). Collectively, the results indicate that the oral administration of tumor Ag plus CT with appropriate mucosal boosting may induce a remarkable suppression of already established tumor growth in the skin via mucosally generated CTLs.

Infiltration of CD8$\alpha\beta$-positive cells in suppressed tumor tissues

We thus examined whether OVA-specific CD8$\alpha\beta$-positive CTLs were actually seen in suppressed tumor tissues such as the stomach and dermis. To determine tumor-infiltrating CD8$\alpha\beta^+$ cells, immunohistochemical staining was performed using biotin-conjugated rat anti-CD8β Ab (Fig. 6*A*, *c* and *g* and *B*, *c* and *g*) or control isotype-matched rat IgG2a Ab (Fig. 6*A*, *d* and *h* and *B*, *d* and *h*). Indeed, although mononuclear cells were seen in the gastric tumor tissues of mice treated with OVA alone, CD8$\alpha\beta$-positive cells were not observed at all (Fig. 6*A*, *a–d*). In contrast, infiltration of inflammatory mononuclear cells together with CD8$\alpha\beta$-positive cells was observed in suppressed gastric tumor tissues (Fig. 6*Ag*). As shown in Fig. 6*Ai*, normal gastric tissue is composed of the epithelium, lamina propria, lamina muscularis mucosae, muscle layer, and serosa from the inside surface in sequence. As compared with normal gastric tissue, a great number of large tumor cells (EG.7-OVA) were mainly found between the lamina muscularis mucosae and serosa of tumor-implanted tissues (Fig. 6*A*, *a* and *b*) and the infiltration of tumor cells into the lamina propria over the lamina muscularis mucosae was also observed (data not shown). However, in suppressed gastric tumor tissues (Fig. 6*Ae*) the tumor cell layer under the lamina muscularis mucosae was markedly thinner than that of an unsuppressed tumor (Fig. 6*Aa*), in which

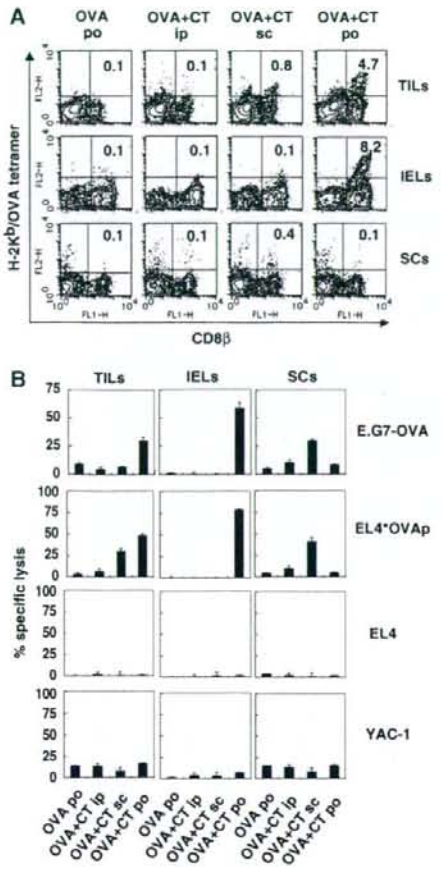

FIGURE 7. Detection of OVA-specific CTLs in TILs. C57BL/6 mice were implanted intradermally with E.G7-OVA cells. Three days later, mice were orally (po), subcutaneously (sc), or intraperitoneally (ip) administered OVA plus CT or orally treated with OVA. Seven days later, the second oral administration was performed in the same manner. TILs, IELs, and SCs were collected from mice 3 days after the second oral administration. *A*, TILs, IELs and SCs were double stained with PE-labeled H-2K^b/OVA tetramer and FITC-labeled anti-mouse CD8β. *B*, OVA-specific CTL responses of TILs, IELs, and SCs were measured by a ^{51}Cr-release assay using E.G7-OVA cells, YAC-1 cells, and EL4 cells pulsed with or without OVA peptide as targets. The E:T ratio is 5:1 in TILs, or 100:1 in IELs and SCs. The results are shown as the mean ± SD in triplicate of pooled cells from three mice. The results are representative of three independent experiments.

tumor cells almost never infiltrated the lamina propria over the lamina muscularis mucosae. Similarly, as for dermal tumor tissues, mononuclear cells together with CD8$\alpha\beta$-positive cells were not observed in mice treated with OVA alone (Fig. 6*B*, *a–d*), whereas the infiltration of a large number of mononuclear cells and CD8$\alpha\beta$-positive cells was observed in suppressed dermal tumor tissues (Fig. 6*B*, *e–g*). Dermal tumor sections were not stained with control isotype-matched rat IgG (Fig. 6*B*, *d* and *h*). As shown in Fig. 6*Bi*, normal skin is composed of epidermides and dermis from the surface in sequence. In tumor cell-implanted dermal tissues, although the infiltration of mononuclear cells or CD8$\alpha\beta$-positive cells was not observed, many large tumor cells were found thickly beneath the epidermides (Fig. 6*B*, *a* and *b*); however, when tumor cell-implanted mice were treated with OVA plus CT, most tumor cells became necrotic or apoptotic (Fig. 6*B*, *e* and *f*).

Measurement of tumor-specific cytotoxic activity by tumor-infiltrating cells in tumor-suppressed mice

To confirm whether infiltrated CD8$\alpha\beta$-positive T cells achieved OVA-specific cytotoxicity, we isolated TILs containing both mononuclear cells and CD8$\alpha\beta$-positive T cells from suppressed dermal tumor tissues as well as from their IELs and SCs. As expected, the number of H-2K^b/OVA tetramer-positive cells increased in both the TILs and IELs but not in the SCs of mice bearing suppressed tumors induced by oral administration with OVA plus CT as compared with mice inoculated with OVA plus CT via another route (Fig. 7*A*), and those increased tetramer-positive cells showed significant direct OVA-specific CTL activity (Fig. 7*B*). It should be noted that, although the number of increased cells specific for the H-2K^b/OVA tetramer was small in mice inoculated with OVA plus CT s.c., both the TILs (0.8%) and the SCs (0.4%) but not the IELs (0.1%) of the mice represented a detectable level of direct OVA-specific cytotoxicity (Fig. 7*B*). These findings suggest that s.c. immunization with Ag plus CT may preferably activate systemic (splenic) Ag-specific CTLs rather than local (intraepithelial) CTLs. Moreover, NK cell cytotoxicity determined against YAC-1 cells was not observed in TILs, IELs, and SCs by oral, s.c., or i.p. immunization of OVA plus CT (Fig. 7*B*), indicating that the suppression of tumor growth was mainly mediated by CD8$\alpha\beta$ CTLs rather than by NK cell cytotoxicity.

Discussion

In the present study we demonstrated that when OVA plus intact CT was orally administered into mice, direct OVA-specific cytotoxicity was dominantly induced in IELs rather than SCs after the first oral priming, and direct OVA-specific cytotoxicity was remarkably expanded in IELs but not in SCs after oral boosting with the same doses of OVA plus CT. Such OVA-specific CTLs were thymic conventional K^b class I MHC molecule-restricted TCR$\alpha\beta^+$ CD8$\alpha\beta$ T cells (32). Moreover, the growth of the OVA-expressing tumor E.G7-OVA thymoma, established previously either in the stomach or dermis, was significantly suppressed by the oral administration of OVA plus CT. Furthermore, marked infiltration of OVA-specific TCR$\alpha\beta^+$ CD8$\alpha\beta$ CTLs with direct cytotoxicity in reduced tumor tissues was observed. These results suggest that activated CTLs with specific cytotoxicity generated at mucosal compartments by oral administration with OVA plus intact CT may be responsible for already established tumor regression.

The majority of tumor regression studies associated with activation of the immune system have focused on systemic immunity observed in the spleen, lymph nodes, and circulating blood rather than local mucosal immunity seen in gut IELs. Those studies have demonstrated only preventative results for tumor establishment by preadministration of tumor Ag plus a suitable adjuvant. In addition, to our knowledge only one study has been shown to suppress already established tumor growth by activating and expanding tumor infiltrating CD8$^+$ CTLs (23). In that study, i.v. vaccination with DCs prepulsed ex vivo with OVA-CT at day 3 and boosted at day 10 after OVA-expressing E.G7 tumor injection induced complete rejection of a visible tumor within 3 wk after the first treatment. Although the inoculation route and the materials for vaccination were different from ours, the timing of the priming and boosting to induce the suppression of already established tumor growth correlated exactly, suggesting that their methods may also initiate strong mucosal direct cytotoxicity mediated through CD8$^+$ CTLs.

Similar to our findings, they also showed that immunization with OVA-CT but not with CTB-conjugated OVA (OVA-CTB)-prepulsed DCs could successfully induce complete rejection of already established tumor growth, although OVA-CTB-prepulsed DC inoculation prevented tumor establishment but not ongoing tumor growth in the skin. Moreover, they insisted that OVA has to be coupled to CT and should be loaded onto DCs for therapeutic DC vaccination based on the observation that neither OVA-CT nor DCs pulsed with unconjugated OVA plus CT could prevent tumor progression. Nonetheless, our findings shown here apparently indicate that we were able to induce effective suppression of ongoing tumor growth by simple oral administration with unconjugated OVA and CT. These results suggest that we may control already established tumor growth at the surface compartments by activating mucosal $CD8^+$ CTLs via orally administered tumor Ag with a suitable mucosal adjuvant. Also, when OVA-CT is orally administered, the conjugation between OVA and CT may be broken through digestion by enzymes secreted in the gastrointestinal tract. Recently, we have reported that modification of OVA in the gastrointestinal tract is essential for oral tolerance induction against OVA (33). Therefore, it is possible that gastrointestinal digestion or modification of OVA may facilitate the delivery of OVA Ag into DCs, critical APCs for OVA-specific CTL induction.

For the efficient induction of such OVA-specific CTLs in vivo using DCs, Eriksson et al. have reported that OVA-CT-prepulsed DC immunization required at least two DC injections, reflecting the priming/boosting procedure (23); however, we have observed that a single oral administration of OVA plus CT seems sufficient to induce effective CTLs to prevent E.G7-OVA thymoma growth, particularly in the skin. This may be because mucosally activated CTLs through oral immunization may be more potent than systemically activated CTLs to suppress transplanted tumors at the mucosal compartment, and oral administration of OVA plus CT seems more efficient to induce mucosal CTLs than i.v. Ag-loaded DC inoculation. Further studies will be needed to explain the differences.

Although both CT-conjugated-OVA and CTB-conjugated OVA are cross-presented by MHC class I in DCs, only CT-OVA but not CTB-OVA cross-primes OVA-specific $CD8^+$ CTLs in vivo (23, 34). Additionally, DCs pulsed with intact OVA alone cannot cross-present and cross-prime CTLs (23). For the cross-priming of Ag-specific CTLs by Ag-captured immature DCs, maturation signaling via some surface molecules such as TLR-3 in those DCs is essential (35, 36). Although whole CT up-regulates the expression of MHC class II, B7.1, and B7.2 molecules on DCs in vitro, neither CTA nor CTB alone up-regulates the levels of surface markers on DCs (37, 38). Also, the binding of CTB to GM1 on DCs seems necessary to efficiently take up both CT itself and Ag and to induce cross-presentation by MHC class I molecules on DCs, whereas CTA may not be taken up to affect DCs. When DCs from GM1-lacking mice were matured in vitro, CT failed to up-regulate the expression of maturation markers and, thus, the binding of B subunits in CT to GM1 molecules on DCs is essential for the induction of DC maturation (37). It has been reported that CTA is required to not only assist in maturation but also to generate the migration of DCs (39, 40); therefore, CTB-mediated matured DCs can initiate their migration to secondary lymphoid organs and colocalization with naive T cells (38). Indeed, CT-loaded but not CTB-loaded DCs could migrate from marginal zones to T cell zones in the spleen (39) and from the subepithelial dome region to T cell zones in PPs (40); therefore, both CTA and CTB were essential for cross-priming CTLs in vivo and neither CTA nor CTB alone could induce CTLs at various compartments (Fig. 3). Taken together, although the detailed mechanisms of efficient Ag presentation via MHC class I and the maturation and migration of DCs by CT are still unknown, digested OVA might be efficiently captured by immature gut mucosal DCs in the presence of CTB and the captured Ag may be cross-presented by MHC class I during DC maturation and migration in the presence of CTA, resulting in the induction of mucosal class I MHC molecule-restricted CTLs that may cause the regression of previously established tumors.

OVA-specific $CD8^+$ CTLs were induced among not only the IELs but also the LPLs of the stomach, small intestine, and large intestine by oral administration of OVA plus CT, a higher percentage of OVA-specific CD8 CTLs was observed in the stomach, small intestine, and large intestine in order, and more specific CTLs were always detected among IELs than among LPLs (Fig. 4, *E* and *F*). Thus, CTLs are much easier to be induced in the upper and more superficial portions of the gastrointestinal tract when Ags are orally administrated with intact CT.

It has been reported that DCs in gastric mucosa are increased in *Helicobacter pylori* (*Hp*)-infected mice and that the response of DCs and T cells to *Hp* Ag is critical for *Hp*-induced gastritis (41). In the present study, Ag-specific CTLs in the stomach might be generated by mucosally activated DCs in the presence of CT and infiltrate-implanted gastric tumor tissues. It is possible that intestinally activated CTLs might migrate to the tumor-implanted stomach, which might also cause CTL infiltration. Actually, such effector CTLs usually express high levels of $\alpha_4\beta_7$ integrin and can home in to the gastric (42), and small and large intestinal mucosa (43) where mucosal addressin cell-adhesion molecule-1 (MadCAM-1), the ligand of $\alpha_4\beta_7$ integrin, is constitutively expressed by post-capillary endothelial cells in small (44, 45) and large intestinal lamina propria (46). Moreover, the number of gastric $\alpha_4\beta_7^{high}$ T cells increased markedly by oral administration of CT in mice (42). It has also been reported that MAdCAM-1 expression is increased in the gastric mucosa after oral administration with cholera vaccine composed of CTB and formalin-inactivated *V. cholerae* (47); therefore, MadCAM-1-expression in gastric mucosa and the recruitment of effector $\alpha 4\beta 7^{high}$ T cells to gastric mucosa might be enhanced by oral administration of the CT adjuvant and, thus, OVA-specific effector CTLs might efficiently infiltrate the OVA Ag-expressing tumor region in the stomach.

In the present study, we found that the growth of dermally implanted tumors was also suppressed by the oral administration of tumor Ag plus whole intact CT. The actual mechanisms for such suppression remains to be elucidated, but there are at least three distinct possibilities: first, the migration of Ag-specific CTLs from the gastrointestinal tract to the skin; second, the migration of Ag-presenting DCs activated in the mucosal compartments by CT; and third, the migration of both cells from the gastrointestinal tract to the skin at the same time. It has been reported that the levels of CCR4 expression, which is associated with T cell homing to the skin, are increased in gastric T cells by infection with *Hp* in humans (48). Moreover, mucosal DCs that take up Ag might migrate to regional lymph nodes near the dermal tumor and prime the CTLs there, and the CTLs could effectively infiltrate dermal tumor tissue. Indeed, Belyakov et al. demonstrated an opposite mechanism in which skin-derived DCs containing heat-labile enterotoxin of *Escherichia coli* migrated to PPs and induced mucosal CTLs by transcutaneous immunization of an Ag and CT (49). Although the detailed mechanisms of this migration of DCs between skin and mucosa are unknown, they have clearly shown that DCs can migrate between the mucosa and skin. We are currently comparing the alteration of DCs in the mucosal compartment, spleen, and lymph nodes after oral administration of an Ag plus natural CT.

Unfortunately, such natural CT is not an appropriate mucosal adjuvant for human clinical investigation (50); however, studies

using natural CT would provide important and critical information about the effect of CT that would be useful for mucosal immune activation. Based on the findings obtained by using natural CT in a mouse model system, we could establish much safer protocols with a mutant CT (51) that induces adenosine diphosphate ribosylation and cyclic adenosine monophosphate formation, which may prevent severe diarrhea as well as retain adjuvant properties. Taken together, an artificial CT-based vaccine targeting DCs may provide a strategy for efficient CTL induction and avirulent mucosal cancer vaccination.

Our data also indicate that E.G7-OVA tumor growth was suppressed by OVA-specific CTLs but not NK cells (Fig. 7*B*). Vaccination with OVA-CT-pulsed DC protects against E.G7-OVA tumor development in vivo in wild-type, NK-depleted, and CD4-deficient mice but not in CD8-deficient mice (34), indicating that the E.G7-OVA tumor might be controlled by CD8 T cells but not by NK cells or CD4 T cells. In fact, TILs in the suppressed tumor did not show any NK-related cytotoxicity (Fig. 7*B*). Moreover, it has been demonstrated that in vitro pretreatment of NK cells with CT inhibits NK cell killing of tumor (YAC-1 or P815), because G proteins in NK cell membranes are ADP ribosylated with CT and ribosylation inhibits the lysis of tumor cells (52); therefore, NK cells do not seem to be involved in the suppression of E.G7-OVA growth in vivo.

It has been shown that activated CTLs but not naive CTLs can represent antitumor (22) or antivirus (12) responses in vivo. In the present study, already established E.G7 tumor growth can be suppressed only when OVA-specific CTLs that show specific cytotoxicity without requiring in vitro restimulation are induced, particularly in the mucosal compartment. To our knowledge, this is the first demonstration of the visual suppression of already established tumor growth by the simple oral administration of tumor Ag plus mucosal adjuvant. The findings shown in the present study herald a new era for cancer immunotherapy.

Acknowledgments

We thank Dr. Yoshihiro Kumagai and Yoshihiko Norose for useful discussions and advice.

Disclosures

The authors have no financial conflict of interest.

References

1. Franks, L. M., and M. A. Knowles. 2005. What is cancer? In *Introduction to the Cellular and Molecular Biology of Cancer*, 4th Ed. M. A. Knowles and P. J. Selby, eds. Oxford University Press, New York, pp. 1–24.
2. Finn, O. J. 2003. Cancer vaccines: between the idea and the reality. *Nat. Rev. Immunol.* 3: 630–641.
3. Czerkinsky, C., F. Anjuere, J. R. McGhee, A. George-Chandy, J. Holmgren, M. P. Kieny, K. Fujiyashi, J. F. Mestecky, V. Pierrefite-Carle, C. Rask, and J. B. Sun. 1999. Mucosal immunity and tolerance: relevance to vaccine development. *Immunol. Rev.* 170: 197–222.
4. Yuki, Y., and H. Kiyono. 2003. New generation of mucosal adjuvants for the induction of protective immunity. *Rev. Med. Virol.* 13: 293–310.
5. Takahashi, H. 2003. Antigen presentation in vaccine development. *Comp. Immunol. Microbiol. Infect. Dis.* 26: 309–328.
6. Hayday, A., E. Theodoridis, E. Ramsburg, and J. Shires. 2001. Intraepithelial lymphocytes: exploring the third way in immunology. *Nat. Immunol.* 2: 997–1003.
7. Offit, P. A., and K. I. Dudzik. 1989. Rotavirus-specific cytotoxic T lymphocytes appear at the intestinal mucosal surface after rotavirus infection. *J. Virol.* 63: 3507–3512.
8. Chardes, T., D. Buzoni-Gatel, A. Lepage, F. Bernard, and D. Bout. 1994. *Toxoplasma gondii* oral infection induces specific cytotoxic CD8 $\alpha\beta^+$ Thy-1$^+$ gut intraepithelial lymphocytes, lytic for parasite-infected enterocytes. *J. Immunol.* 153: 4596–4603.
9. Muller, S., M. Buhler-Jungo, and C. Mueller. 2000. Intestinal intraepithelial lymphocytes exert potent protective cytotoxic activity during an acute virus infection. *J. Immunol.* 164: 1986–1994.
10. Taunk, J., A. I. Roberts, and E. C. Ebert. 1992. Spontaneous cytotoxicity of human intraepithelial lymphocytes against epithelial cell tumors. *Gastroenterology* 102: 69–75.
11. Roberts, A. I., S. M. O'Connell, L. Biancone, R. E. Brolin, and E. C. Ebert. 1993. Spontaneous cytotoxicity of intestinal intraepithelial lymphocytes: clues to the mechanism. *Clin. Exp. Immunol.* 94: 527–532.
12. Kuribayashi, H., A. Wakabayashi, M. Shimizu, H. Kaneko, Y. Norose, Y. Nakagawa, J. Wang, Y. Kumagai, D. H. Margulies, and H. Takahashi. 2004. Resistance to viral infection by intraepithelial lymphocytes in HIV-1 P18-I10-specific T-cell receptor transgenic mice. *Biochem. Biophys. Res. Commun.* 316: 356–363.
13. Takahashi, H., J. Cohen, A. Hosmalin, K. B. Cease, R. Houghten, J. L. Cornette, C. DeLisi, B. Moss, R. N. Germain, and J. A. Berzofsky. 1988. An immunodominant epitope of the human immunodeficiency virus envelope glycoprotein gp160 recognized by class I major histocompatibility complex molecule-restricted murine cytotoxic T lymphocytes. *Proc. Natl. Acad. Sci. USA* 85: 3105–3109.
14. Williams, N. A., T. R. Hirst, and T. O. Nashar. 1999. Immune modulation by the cholera-like enterotoxins: from adjuvant to therapeutic. *Immunol. Today* 20: 95–101.
15. Lencer, W. I., and B. Tsai. 2003. The intracellular voyage of cholera toxin: going retro. *Trends Biochem. Sci.* 28: 639–645.
16. Elson, C. O., and W. Ealding. 1984. Generalized systemic and mucosal immunity in mice after mucosal stimulation with cholera toxin. *J. Immunol.* 132: 2736–2741.
17. Marinaro, M., H. F. Staats, T. Hiroi, R. J. Jackson, M. Coste, P. N. Boyaka, N. Okahashi, M. Yamamoto, H. Kiyono, H. Bluethmann, et al. 1995. Mucosal adjuvant effect of cholera toxin in mice results from induction of T helper 2 (Th2) cells and IL-4. *J. Immunol.* 155: 4621–4629.
18. Bowen, J. C., S. K. Nair, R. Reddy, and B. T. Rouse. 1994. Cholera toxin acts as a potent adjuvant for the induction of cytotoxic T-lymphocyte responses with non-replicating antigens. *Immunology* 81: 338–342.
19. Carbone, F. R., and M. J. Bevan. 1989. Induction of ovalbumin-specific cytotoxic T cells by in vivo peptide immunization. *J. Exp. Med.* 169: 603–612.
20. Moore, M. W., F. R. Carbone, and M. J. Bevan. 1988. Introduction of soluble protein into the class I pathway of antigen processing and presentation. *Cell* 54: 777–785.
21. Porgador, A., H. F. Staats, B. Faiola, E. Gilboa, and T. J. Palker. 1997. Intranasal immunization with CTL epitope peptides from HIV-1 or ovalbumin and the mucosal adjuvant cholera toxin induces peptide-specific CTLs and protection against tumor development in vivo. *J. Immunol.* 158: 834–841.
22. Dalyot-Herman, N., O. F. Bathe, and T. R. Malek. 2000. Reversal of CD8$^+$ T cell ignorance and induction of anti-tumor immunity by peptide-pulsed APC. *J. Immunol.* 165: 6731–6737.
23. Eriksson, K., J. B. Sun, I. Nordstrom, M. Fredriksson, M. Lindblad, B. L. Li, and J. Holmgren. 2004. Coupling of antigen to cholera toxin for dendritic cell vaccination promotes the induction of MHC class I-restricted cytotoxic T cells and the rejection of a cognate antigen-expressing model tumor. *Eur. J. Immunol.* 34: 1272–1281.
24. Taguchi, T., J. R. McGhee, R. L. Coffman, K. W. Beagley, J. H. Eldridge, K. Takatsu, and H. Kiyono. 1990. Analysis of Th1 and Th2 cells in murine gut-associated tissues: frequencies of CD4$^+$ and CD8$^+$ T cells that secrete IFN-γ and IL-5. *J. Immunol.* 145: 68–77.
25. Takahashi, M., E. Osono, Y. Nakagawa, J. Wang, J. A. Berzofsky, D. H. Margulies, and H. Takahashi. 2002. Rapid induction of apoptosis in CD8$^+$ HIV-1 envelope-specific murine CTLs by short exposure to antigenic peptide. *J. Immunol.* 169: 6588–6593.
26. Semple, J. W., and M. R. Szewczuk. 1986. Natural killer cells in murine muscular dystrophy: IV. Characterization of Percoll fractionated splenic and thymic natural killer cells and natural killer-sensitive thymocyte targets. *Clin. Immunol. Immunopathol.* 41: 116–129.
27. Belz, G. T., W. Xie, and P. C. Doherty. 2001. Diversity of epitope and cytokine profiles for primary and secondary influenza a virus-specific CD8$^+$ T cell responses. *J. Immunol.* 166: 4627–4633.
28. Nakatsuka, K., H. Sugiyama, Y. Nakagawa, and H. Takahashi. 1999. Purification of antigenic peptide from murine hepatoma cells recognized by class-I major histocompatibility complex molecule-restricted cytotoxic T-lymphocytes induced with B7-1-gene-transfected hepatoma cells. *J. Hepatol.* 30: 1119–1129.
29. Kilshaw, P. J., and K. C. Baker. 1988. A unique surface antigen on intraepithelial lymphocytes in the mouse. *Immunol. Lett.* 18: 149–154.
30. Russell, G. J., C. M. Parker, K. L. Cepek, D. A. Mandelbrot, A. Sood, E. Mizoguchi, E. C. Ebert, M. B. Brenner, and A. K. Bhan. 1994. Distinct structural and functional epitopes of the α E β 7 integrin. *Eur. J. Immunol.* 24: 2832–2841.
31. Lefrancois, L., T. A. Barrett, W. L. Havran, and L. Puddington. 1994. Developmental expression of the α IEL β 7 integrin on T cell receptor γ δ and T cell receptor α β T cells. *Eur. J. Immunol.* 24: 635–640.
32. Rocha, B., P. Vassalli, and D. Guy-Grand. 1994. Thymic and extrathymic origins of gut intraepithelial lymphocyte populations in mice. *J. Exp. Med.* 180: 681–686.
33. Wakabayashi, A., Y. Kumagai, E. Watari, M. Shimizu, M. Utsuyama, K. Hirokawa, and H. Takahashi. 2006. Importance of gastrointestinal ingestion and macromolecular antigens in the vein for oral tolerance induction. *Immunology* 119: 167–177.
34. Sun, J. B., K. Eriksson, B. L. Li, M. Lindblad, J. Azem, and J. Holmgren. 2004. Vaccination with dendritic cells pulsed in vitro with tumor antigen conjugated to cholera toxin efficiently induces specific tumoricidal CD8$^+$ cytotoxic lymphocytes dependent on cyclic AMP activation of dendritic cells. *Clin. Immunol.* 112: 35–44.

35. Fujimoto, C., Y. Nakagawa, K. Ohara, and H. Takahashi. 2004. Polyriboinosinic polyribocytidylic acid [poly(I:C)]/TLR3 signaling allows class I processing of exogenous protein and induction of HIV-specific CD8$^+$ cytotoxic T lymphocytes. *Int. Immunol.* 16: 55–63.
36. Schulz, O., S. S. Diebold, M. Chen, T. I. Naslund, M. A. Nolte, L. Alexopoulou, Y. T. Azuma, R. A. Flavell, P. Liljestrom, and C. Reis e Sousa. 2005. Toll-like receptor 3 promotes cross-priming to virus-infected cells. *Nature* 433: 887–892.
37. Kawamura, Y. I., R. Kawashima, Y. Shirai, R. Kato, T. Hamabata, M. Yamamoto, K. Furukawa, K. Fujihashi, J. R. McGhee, H. Hayashi, and T. Dohi. 2003. Cholera toxin activates dendritic cells through dependence on GM1-ganglioside which is mediated by NF-κB translocation. *Eur. J. Immunol.* 33: 3205–3212.
38. Gagliardi, M. C., F. Sallusto, M. Marinaro, A. Langenkamp, A. Lanzavecchia, and M. T. De Magistris. 2000. Cholera toxin induces maturation of human dendritic cells and licences them for Th2 priming. *Eur. J. Immunol.* 30: 2394–2403.
39. Grdic, D., L. Ekman, K. Schon, K. Lindgren, J. Mattsson, K. E. Magnusson, P. Ricciardi-Castagnoli, and N. Lycke. 2005. Splenic marginal zone dendritic cells mediate the cholera toxin adjuvant effect: dependence on the ADP-ribosyltransferase activity of the holotoxin. *J. Immunol.* 175: 5192–5202.
40. Shreedhar, V. K., B. L. Kelsall, and M. R. Neutra. 2003. Cholera toxin induces migration of dendritic cells from the subepithelial dome region to T- and B-cell areas of Peyer's patches. *Infect. Immun.* 71: 504–509.
41. Drakes, M. L., S. J. Czinn, and T. G. Blanchard. 2006. Regulation of murine dendritic cell immune responses by *Helicobacter felis* antigen. *Infect. Immun.* 74: 4624–4633.
42. Michetti, M., C. P. Kelly, J. P. Kraehenbuhl, H. Bouzourene, and P. Michetti. 2000. Gastric mucosal $\alpha_4\beta_7$-integrin-positive CD4 T lymphocytes and immune protection against *Helicobacter* infection in mice. *Gastroenterology* 119: 109–118.
43. Lefrancois, L., C. M. Parker, S. Olson, W. Muller, N. Wagner, M. P. Schon, and L. Puddington. 1999. The role of β_7 integrins in CD8 T cell trafficking during an antiviral immune response. *J. Exp. Med.* 189: 1631–1638.
44. Berlin, C., R. F. Bargatze, J. J. Campbell, U. H. von Andrian, M. C. Szabo, S. R. Hasslen, R. D. Nelson, E. L. Berg, S. L. Erlandsen, and E. C. Butcher. 1995. α_4 integrins mediate lymphocyte attachment and rolling under physiologic flow. *Cell* 80: 413–422.
45. Berlin, C., E. L. Berg, M. J. Briskin, D. P. Andrew, P. J. Kilshaw, B. Holzmann, I. L. Weissman, A. Hamann, and E. C. Butcher. 1993. $\alpha_4\beta_7$ integrin mediates lymphocyte binding to the mucosal vascular addressin MAdCAM-1. *Cell* 74: 185–195.
46. Streeter, P. R., E. L. Berg, B. T. Rouse, R. F. Bargatze, and E. C. Butcher. 1988. A tissue-specific endothelial cell molecule involved in lymphocyte homing. *Nature* 331: 41–46.
47. Lindholm, C., A. Naylor, E. L. Johansson, and M. Quiding-Jarbrink. 2004. Mucosal vaccination increases endothelial expression of mucosal addressin cell adhesion molecule 1 in the human gastrointestinal tract. *Infect. Immun.* 72: 1004–1009.
48. Lundgren, A., C. Trollmo, A. Edebo, A. M. Svennerholm, and B. S. Lundin. 2005. *Helicobacter pylori*-specific CD4$^+$ T cells home to and accumulate in the human *Helicobacter pylori*-infected gastric mucosa. *Infect. Immun.* 73: 5612–5619.
49. Belyakov, I. M., S. A. Hammond, J. D. Ahlers, G. M. Glenn, and J. A. Berzofsky. 2004. Transcutaneous immunization induces mucosal CTLs and protective immunity by migration of primed skin dendritic cells. *J. Clin. Invest.* 113: 998–1007.
50. Clarke, L. L., B. R. Grubb, S. E. Gabriel, O. Smithies, B. H. Koller, and R. C. Boucher. 1992. Defective epithelial chloride transport in a gene-targeted mouse model of cystic fibrosis. *Science* 257: 1125–1128.
51. Yamamoto, S., Y. Takeda, M. Yamamoto, H. Kurazono, K. Imaoka, M. Yamamoto, K. Fujihashi, M. Noda, H. Kiyono, and J. R. McGhee. 1997. Mutants in the ADP-ribosyltransferase cleft of cholera toxin lack diarrheagenicity but retain adjuvanticity. *J. Exp. Med.* 185: 1203–1210.
52. Maghazachi, A. A., A. Al-Aoukaty, C. Naper, K. M. Torgersen, and B. Rolstad. 1996. Preferential involvement of Go and Gz proteins in mediating rat natural killer cell lysis of allogeneic and tumor target cells. *J. Immunol.* 157: 5308–5314.

Available online at www.sciencedirect.com
ScienceDirect
Virology 367 (2007) 390–397
VIROLOGY
www.elsevier.com/locate/yviro

Chimeric adenovirus type 5/35 vector encoding SIV *gag* and HIV *env* genes affords protective immunity against the simian/human immunodeficiency virus in monkeys

Kenji Someya [a,b,c,*], Ke-Qin Xin [c], Yasushi Ami [d], Yasuyuki Izumi [b], Hiroyuki Mizuguchi [e], Shinrai Ohta [b,c], Naoki Yamamoto [b], Mitsuo Honda [b], Kenji Okuda [c]

[a] *Department of Virology III, National Institute of Infectious Diseases, Musashimurayama, Tokyo 208-0011, Japan*
[b] *AIDS Research Center, National Institute of Infectious Diseases, Shinjuku-ku, Tokyo 162-8640, Japan*
[c] *Department of Molecular Biodefense Research, Yokohama City University, School of Medicine, Kanazawa-ku Yokohama 236-0004, Japan*
[d] *Division of Experimental Animal Research, National Institute of Infectious Diseases, Musashimurayama, Tokyo 208-0011, Japan*
[e] *Laboratory of Gene Transfer and Regulation, National Institute of Biomedical Innovation, Ibaraki, Osaka 567-0085, Japan*

Received 29 March 2007; returned to author for revision 30 April 2007; accepted 14 June 2007
Available online 12 July 2007

Abstract

Replication-defective adenovirus type 5 (Ad5) vector-based vaccines are widely known to induce strong immunity against immunodeficiency viruses. To exploit this immunogenicity while overcoming the potential problem of preexisting immunity against human adenoviruses type 5, we developed a recombinant chimeric adenovirus type 5 with type 35 fiber vector (rAd5/35). We initially produced a simian immunodeficiency virus (SIV) *gag* DNA plasmid (rDNA-Gag), a human immunodeficiency virus type 1 (HIV-1) 89.6 *env* DNA plasmid (rDNA-Env) and a recombinant Ad5/35 vector encoding the SIV *gag* and HIV *env* gene (rAd5/35-Gag and rAd5/35-Env). Prime-boost vaccination with rDNA-Gag and -Env followed by high doses of rAd5/35-Gag and -Env elicited higher levels of cellular immune responses than did rDNAs or rAd5/35s alone. When challenged with a pathogenic simian human immunodeficiency virus (SHIV), animals receiving a prime-boost regimen or rAd5/35s alone maintained a higher number of $CD4^+$ T cells and remarkably suppressed plasma viral RNA loads. These findings suggest the clinical promise of an rAd5/35 vector-based vaccine.

Keywords: DNA vaccine; Recombinant Ad5/35; Cellular immunity; Pathogenic SHIV challenge

Introduction

HIV-specific cellular and humoral responses play a critical role in controlling viral replication and disease progression (Mascola, 2003; Letvin et al., 2002; Musey et al., 1997). It has been reported that recombinant live virus- and bacteria-based vaccines such as recombinant adenovirus (Mascola et al., 2005; Shiver et al., 2002) recombinant poxvirus (Someya et al., 2004; Amara et al., 2001), and recombinant BCG (Ami et al., 2005; Someya et al., 2005) elicited high levels of effective immunity against immunodeficiency viruses when used either alone or in conjunction with other vectors.

Adenoviruses, which are associated with benign pathologies in humans, are attractive for use in HIV vaccines because their genome has been extensively studied and because methods for constructing recombinant vectors with them are well established (Imler, 1995). A regimen that primes with DNA and then boosts with rAd5 is known to protect macaques against SHIV challenge by inducing high levels of viral-specific immunities (Shiver et al., 2002). However, Ad5 has been prevented from fully realizing its clinical potential (Catanzaro et al., 2006) because of preexisting humoral immunity to adenoviruses (Barouch et al., 2004; Casimiro et al., 2003). A previous study demonstrated that neutralizing antibodies against Ad5 are widespread in healthy blood donors in the developed world, whereas neutralizing

* Corresponding author. Department of Virology III, National Institute of Infectious Diseases 4-7-1 Gakuen, Musashimurayama, Tokyo 208-0011, Japan. Fax: +81 42 565 3315.
E-mail address: someyan@nih.go.jp (K. Someya).

0042-6822/$ - see front matter © 2007 Elsevier Inc. All rights reserved.
doi:10.1016/j.virol.2007.06.012

antibodies against Ad35 are rare (Kostense et al., 2004; Vogels et al., 2003). Furthermore, patients at risk of AIDS were reported to have a much higher seroprevalence of Ad5 than Ad35 (Kostense et al., 2004).

We have recently constructed an adenovirus serotype 5 vector that possesses serotype 35 fiber (rAd5/35) that encodes the simian immunodeficiency virus (SIV) *gag* gene or human immunodeficiency virus type 1 (HIV-1) IIIB *env* gp160 gene (Xin et al., 2005). The rAd5/35 vector, which lacks the E1 and E3 genes that are responsible for viral replication (Imler, 1995), interacts with CD46-expressing cells (Gaggar et al., 2003) and antigen-presenting cells (Rea et al., 2001). The rAd5/35 vector was shown to enter human dendritic cells (DC) more efficiently than Ad5 and activate T cells *ex vivo* (Ophorst et al., 2004), suggesting that a rAd5/35 vector-based vaccine may be an effective activator for T cell immunity. However, rAd5/35 vector-expressing measles virus hemagglutinin was less immunogenic than rAd5 in low-dose immunization in macaques and suggested that fiber exchange may not circumvent anti-Ad5 immunity during acute Ad5 infection in mice (Ophorst et al., 2004).

Recently, hyper variable regions on the Ad5 hexon protein were successfully replaced with those of the rare Ad48, allowing preexisting anti-vector immunity to be circumvented (Roberts et al., 2006). We previously showed that, when combined with plasmid DNA, the rAd5/35 vector elicited high levels of cellular responses that in turn protected mice from challenge with a virulent vaccinia virus encoding HIV-1 BH8 env (Xin et al., 2005). Furthermore, the rAd5/35 vector-based vaccine was not affected by the preexisting anti-Ad5 immunity in mice.

These results suggest that a vaccine combining plasmid DNA and the rAd5/35 vector may induce effective viral-specific immunities in macaques. In this study, we determined the vaccine efficacy of relatively high doses of rAd5/35 vector-based HIV vaccine in an SHIV macaque model.

Results

Vaccine-induced T cell responses to SIV Gag and HIV Env

After priming with rDNA-Gag and rDNA-Env, Gag- and Env-specific IFN-γ spot-forming cells (SFC) were detected in both the rDNA and the prime-boost groups (Fig. 1A). The numbers of SFC against Gag peaked at 16 weeks in the rDNA and the prime-boost groups, with numbers averaging 120 in the rDNA group and 128 in the prime-boost group. ELISPOT responses to Env also peaked at 16 weeks, with average numbers of 33 in the rDNA group and of 66 in the prime-boost group. Gag- and Env-specific ELISPOT responses were not observed in animals immunized with cDNA (SFC ≤ 10).

Two serial high-dose injections with rAd5/35-Gag and rAd5/35-Env per animal dramatically augmented Gag- and Env-specific ELISPOT responses in the prime-boost group (Fig. 1A). At Week 150, the prime-boost group averaged 53 Gag-specific and 35 Env-specific SFC. Two weeks after the two serial injections with rAd5/35 (154 weeks), the average number of Gag-specific SFC increased to 1073 and that of Env-specific SFC to 340. Two serial injections with rAd5/35s also elicited higher ELISPOT responses in the rAd5/35 group (Fig. 1A), with the average number of Gag-specific SFC increasing from 35 to 570 and that of Env-specific SFC, from 15 to 165. The levels of both Gag and Env ELISPOT responses at the time of virus challenge (154 weeks) significantly increased in the prime-boost group, and they were higher than those in the rDNA (Gag, $p<0.01$; ENV, $p<0.01$) and the cDNA (Gag, $p<0.01$; Env, $p<0.01$) groups. Serial injections with cAd5/35s failed to enhance responses to Gag or Env in either the rDNA or the cDNA group.

Vaccine-induced antibody responses to SIV Gag and HIV Env

Both anti-Gag- and Env-specific IgG responses were detected after serial inoculations with rDNA-Gag and rDNA-Env (Fig. 1B). Anti-Gag-specific IgG titers peaked at 16 weeks in the rDNA group, averaging 123 and at 32 weeks in the prime-boost group, averaging 155 (Fig. 1B, upper panel). The anti-Env-specific IgG titers for both the rDNA and the prime-boost groups peaked at 32 weeks, with titers of 200 and 183, respectively (Fig. 1B, lower panel). Two serial injections with rAd5/35-Gag and rAd5/35-Env to the prime-boost group enhanced both anti-Gag- and anti-Env-specific IgG titers, with the former increasing from an average of 100 at 150 weeks to an average of 823 at 154 weeks and the latter increasing from an average of 74 at 150 weeks to 2240 at 154 weeks. Two serial injections with rAd5/35-Gag and rAd5/35-Env to the rAd5/35 group generated both anti-Gag- and anti-Env-specific IgG responses, with the peak titers in the former averaging 335 and in the latter, 480. Both the anti-Gag- and Env-specific IgG titers at the time of virus challenge (154 weeks) in the prime-boost group were significantly higher than those in the rDNA (Gag, $p<0.01$; Env, $p<0.01$) and the cDNA (Gag, $p<0.01$; Env, $p<0.01$) groups. When anti-HIV-89.6-specific neutralization antibody responses were measured at 154 weeks using the purified serum IgG, the rDNA, the rAd35 and the prime-boost groups showed an average neutralization of 4%, 10% and 24% respectively (data not shown), suggesting that the antibody may not contribute to the partial protection from virus challenge in monkeys. Two serial injections with Ad5/35-LacZ had no effect on anti-Gag and anti-Env IgG responses.

Plasma viral RNA loads and $CD4^+$ T cell counts after challenge with SHIV

To evaluate the efficacy of a prime-boost vaccine regimen, all animals received an intravenous challenge with 20 $TCID_{50}$ of highly pathogenic SHIV at 154 weeks (Table 1). Peak plasma RNA loads (Fig. 2A) and rapid or transient $CD4^+$ T cell loss (Fig. 2B) were observed within 2 weeks after challenge (acute phase). The cDNA group had the greatest viral RNA loads (peaking at an average of 4.5×10^9 copies/ml) and experienced dramatic loss of $CD4^+$ T cells (≤ 50 cells/μl). Although its peak viral RNA loads (an average of 4.9×10^8 copies/ml) were almost ten-fold less than those of the cDNA group ($p<0.01$), the rDNA group likewise showed reduced $CD4^+$ T cell numbers

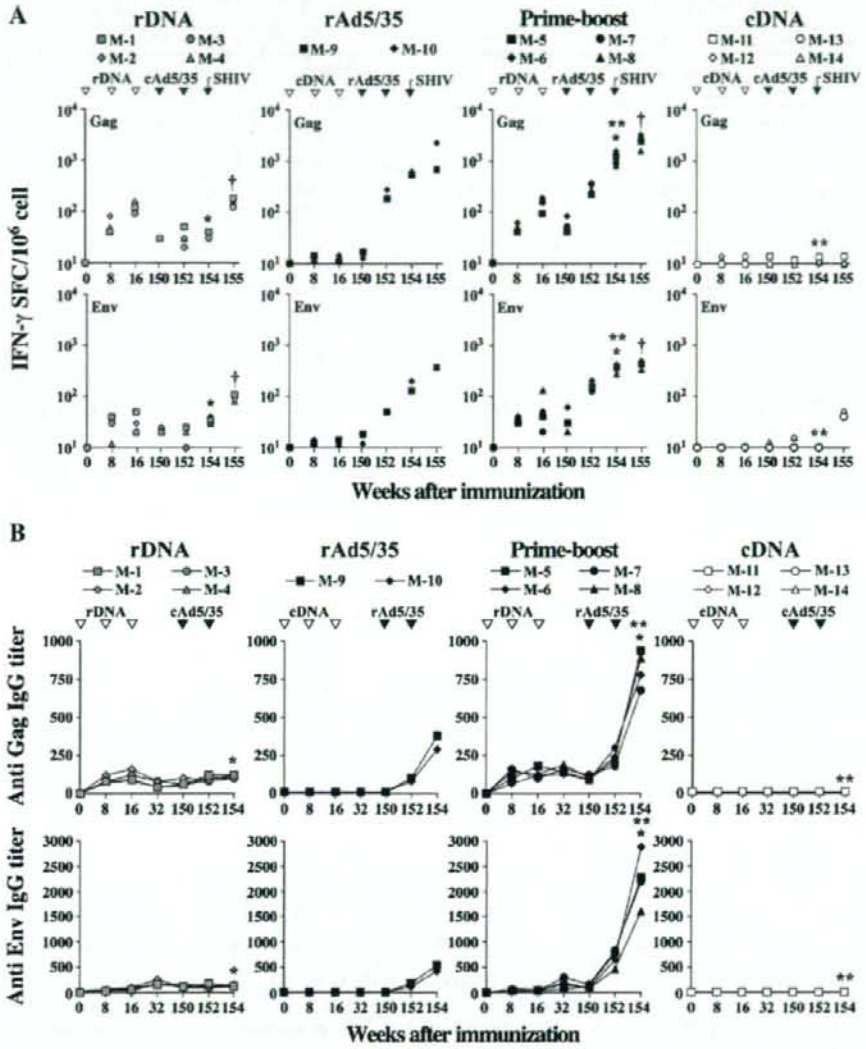

Fig. 1. Cellular and humoral responses of vaccinated animals. (A) Freshly isolated PBMC were stimulated with SIV Gag and HIV Env peptides. An ELISPOT assay was used to monitor the numbers of antigen-specific IFN-γ spot-forming cells. *rDNA vs. prime-boost, $p<0.01$ (154 weeks). **Prime-boost vs. cDNA, $p<0.01$ (154 weeks). †rDNA vs. prime-boost group, $p<0.01$ (155 weeks). (B) End-point Gag- and Env-specific plasma IgG titers were determined in the course of immunization using ELISA. *rDNA vs. prime-boost, $p<0.01$ (154 weeks). **Prime-boost vs. cDNA, $p<0.01$ (154 weeks).

(≤40 cells/μl, no significance). The prime-boost group showed greater than 600-fold reduction in peak viral loads and maintained higher $CD4^+$ T cell numbers compared to the cDNA group (the peak viral loads of the prime-boost group in the acute viral phase: an average of 7.3×10^6 copies/ml, $p<0.01$; $CD4^+$ T cell numbers of the prime-boost group: an average of 616 cells/μl, $p<0.01$). The initial viremia and $CD4^+$ T cell numbers in the prime-boost group were also significantly lower than those in the rDNA group (peak viral RNA loads, $p<0.01$; $CD4^+$ T cell numbers, $p<0.01$). The rAd5/35 group showed 600-fold reduction in the peak viral loads (an average of 5.3×10^6 copies/ml) compared to the cDNA group and maintained higher $CD4^+$ T cell numbers (an average of 500 cells/μl).

During the set-point phase, the cDNA group showed higher viral RNA loads (≥5×10^6 copies/ml) and lower $CD4^+$ T cell numbers (≤20 cells/μl) (Fig. 2). The set-point viral RNA loads of the rDNA group (averaging 10^6 copies/ml) were approximately five-fold lower than those of the control group, but the $CD4^+$ T cell numbers recovered by no more than 100 cells/μl. Two animals (M-5 and M-6) of the prime-boost group showed well-controlled set-point viral loads and minimal $CD4^+$ T cells

Table 1
Immunization and challenge schedule

Group (regimen)	Monkey no.	Priming immunization and route	Schedule (week of priming)	Booster immunization and route	Schedule (week of boosting)	SHIV challenge
rDNA	M-1, M-2, M-3, M-4	rDNA-Gag, 2.5 mg, i.m. and rDNA-Env, 2.5 mg, i.m.	0, 8, 16	cAd5/35, 2×10^{11} vp, i.d.	150, 152	20 $TCID_{50}$, i.v., Week 154
Prime-boost	M-5, M-6, M-7, M-8	rDNA-Gag, 2.5 mg, i.m. and rDNA-Env, 2.5 mg, i.m.	0, 8, 16	rAD3/35-Gag, 10^{11} vp, i.d. and rAD3/35-Env, 10^{11} vp, i.d.	150, 152	20 $TCID_{50}$, i.v., Week 154
rAd5/35	M-9, M-10	cDNA, 5 mg, i.m.	0. 8, 16	rAD3/35-Gag, 10^{11} vp, i.d. and rAD3/35-Env, 10^{11} vp, i.d.	150, 152	20 $TCID_{50}$, i.v., Week 154
cDNA	M-11, M-12, M-13, M-14	cDNA, 5 mg, i.m.	0. 8, 16	cAd5/35, 2×10^{11} vp, i.d.	150, 152	20 $TCID_{50}$, i.v., Week 154

loss, while the other two macaques (M-7 and M-8) of the same group showed slightly higher viral RNA loads and lower $CD4^+$ T cell numbers. The set-point viral RNA loads for M-6 were within the detection limit (500 copies/ml) and those for M-5 ranged from <500 to 3×10^3 copies/ml. The viremia-controlled M-6 showed more than 800 $CD4^+$ T cells/μl and M-5 showed 600 cells/μl, with the exception of the transient loss (about 350 cells/μl) occurring at 6 and 18 weeks. Set-point viral RNA loads for both M-7 and M-8 ranged from 3.7×10^3 to 4.2×10^4 copies/ml, while $CD4^+$ T cell numbers ranged from 300 to 600 cells/μl. Of the two macaques in the rAd5/35 group, one showed enhanced protection, while the other did not. M-9 suppressed viral loads to less than 10^4 copies/ml and maintained $CD4^+$ T cell numbers at levels of more than 500 cells/μl. The viral loads for M-10 ranged from 10^5 to 10^6 copies/ml, and its $CD4^+$ T cell numbers were less than 300 cells/μl. Throughout the set-point phase, average plasma viral RNA loads and $CD4^+$ T cell numbers in the prime-boost group were significantly different compared to those in the cDNA (plasma viral RNA loads, $p<0.01$; $CD4^+$ T cell numbers, $p<0.01$) and rDNA (plasma viral RNA loads, $p<0.01$; $CD4^+$ T cell numbers, $p<0.01$) groups.

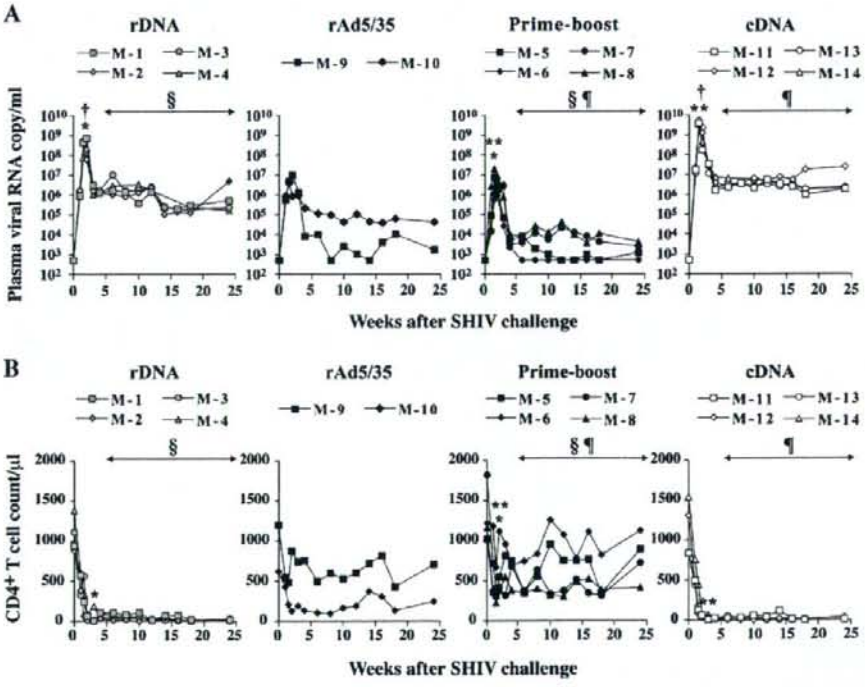

Fig. 2. Plasma viral RNA loads and $CD4^+$ T cell counts after challenge with SHIV. (A) Plasma RNA copies were determined by quantitative RT-PCR with a detection limit of 500 viral RNA copies per ml. *rDNA vs. prime-boost, $p<0.01$ (acute phase). **Prime-boost vs. cDNA, $p<0.01$ (acute phase). †rDNA vs. cDNA, $p<0.01$ (acute phase). §rDNA vs. prime-boost, $p<0.01$ (set-point phase). ¶Prime-boost vs. cDNA, $p<0.01$ (set-point phase). (B) Whole blood was stained with CD3 and CD4 antibodies. $CD4^+$ T cell numbers were determined using flow cytometry. *rDNA vs. prime-boost, $p<0.01$ (acute phase). **Prime-boost vs. cDNA, $p<0.01$ (acute phase). §rDNA vs. prime-boost, $p<0.01$ (set-point phase). ¶Prime-boost vs. cDNA, $p<0.01$ (set-point phase).

T cells immune response to Gag and Env after challenge with SHIV

At an early phase of infection (1 week after challenge), IFN-γ ELISPOT responses showed that the prime-boost group had higher numbers of Gag- and Env-specific SFC (Gag specific, an average of 2385; Env specific, an average of 420) than those of the rAd5/35 group (Gag specific, an average of 920; Env specific, an average of 270) (Fig. 2A). Furthermore, lower numbers of SFC were seen in the rDNA group (an average of 153 SFC specific for Gag; an average of 103 SFC specific for Env) than those in the prime-boost group (Gag, $p<0.01$; Env, $p<0.01$). The cDNA group showed no responses (≤ 30 SFC). Taken together, these results suggest that the prime-boost regimen elicited the highest frequency of cellular memory T cells in response to viral challenge.

Discussion

Higher plasma viral RNA loads and lower $CD4^+$ T cell numbers have been linked to disease progression in HIV-infected individuals (Patke et al., 2002; Mellors et al., 1996, 1997), suggesting that the generation of robust HIV-specific immunity may be critical in the control of viral infection. Recently, it was shown that a recombinant Ad5 vector-based HIV vaccine induced high levels of cellular immunity and protected animals from highly pathogenic viral challenge (Shiver et al., 2002). In contrast, other studies have shown that preexisting anti-Ad5 immunity can attenuate the efficacy of recombinant Ad5-based HIV vaccine (Barouch et al., 2004; Kostense et al., 2004; Casimiro et al., 2003). It is essential that such preexisting anti-Ad5 immunity be overcome if we are to enjoy the benefits offered by Ad5 as a vaccine vector, such as its induction of strong T cell immunity. Rare serotype Ad35, which is classified into subgroup B, has different cell tropism from Ad5 (Marttila et al., 2005; Segerman et al., 2000; Shayakhmetov et al., 2000; De Jong et al., 1997), and the seroprevalence of Ad35 in immunocompromised individuals and those at risk of AIDS was lower than that of Ad5, suggesting that Ad35 could be used as the base for an HIV vaccine (Kostense et al., 2004; Vogels et al., 2003). Therefore, the advantage of constructing a chimeric Ad5/35 vaccine is that the vector will retain its infectivity with less risk of preexisting immunity against the vaccine vector than that of Ad5-based vaccine. This suggests that the Ad5/35 vaccine would allow the basis for adenoviral vectors to be broadened with improved properties.

In this study, we initially constructed Ad5/35 vector-based HIV vaccine and demonstrated that its immunogenicity and protective efficacy in a macaque model. The rAd5/35 vector was previously developed as a vaccine vehicle for DC targeting (Xin et al., 2005, 2007; Mizuguchi and Hayakawa, 2002), and the rAd5/35 vector showed much lower hepatotoxicity than Ad5 (Xin et al., 2005). Recently, Ophorst et al. (2004) reported that rAd5 vector carrying a part of the fiber molecule of Ad35 (rAd5. Fib35) was less immunogenic in monkeys than rAd5, and rAd5. Fib35 showed no significant difference in anti-insert immunity over Ad5 in mice with high Ad5 vector-specific immunity. In addition, Abbink et al. (2007) reported comparative seroprevalence and immunogenicity studies involving rAd11, rAd35 and rAd50 vectors from subgroup B, rAd26, rAd48 and rAd49 vectors from subgroup D and rAd5 vectors from subgroup C. These rAd vectors were rare serotypes and elicited Gag-specific cellular immune responses in mice both with and without anti-Ad5 immunity. However, the rare serotype-based rAd vectors have proven less immunogenic than rAd5 vectors in animal models in spite of the absence of anti-Ad5 immunity (Barouch et al., 2004; Lemckert et al., 2005). In our previous study, rAd5/35 vector was highly immunogenic and significantly less susceptible to preexisting anti-Ad5 immunity than a comparable Ad5 vector (Xin et al., 2005). Although we did not compare the rAd5/35 vector directly with other serotype rAd vectors, we demonstrated that the rAd5/35 vector was immunogenic, and a much higher degree of immunogenicity was achieved by adopting a prime-boost regimen combining rAd5/35 vectors with rDNA vaccine in macaques.

To evaluate the efficacy of the vaccine, we monitored T cell responses, plasma viral RNA loads and $CD4^+$ T cell numbers following SHIV challenge. In the present study, we used highly pathogenic SHIV-C2/1 (Shinohara et al., 1998), which originated from SHIV 89.6 (Lu et al., 1996; Reimann et al., 1996) because our vaccine regimen was designed to target SIV Gag and HIV Env antigens and for the virus to well reproduce high plasma viremia and loss of $CD4^+$ cells (Eda et al., 2006; Someya et al., 2005, 2006; Ami et al., 2005; Shinohara et al., 1998).

After challenge with SHIV, all animals in the prime-boost and the rAd5/35 groups showed high memory T cell responses against Gag and Env, and these animals showed a reduction in peak viral RNA loads at the acute phase of infection. Furthermore, in the set-point phase, two animals in the prime-boost group and one animal in the rAd5/35 group controlled SHIV infection, and the remaining two animals in the prime-boost and one animal in the rAd5/35 groups showed moderate control. In spite of higher cellular responses being observed in the prime-boost group than those in the rAd5/35 group, the difference in protective levels between the prime-boost and the rAd5/35 groups was not clearly separated. Although it is not possible to directly compare the levels of immune responses and protective efficacy induced by the rAd5/35 vector to those of other rAd vector studies, our results appeared to be similar to those obtained with the other rAds (Abbink et al., 2007; Barratt-Boyes et al., 2006; Ophorst et al., 2004; Shiver et al., 2002; Musey et al., 1997). To clarify the efficacy of the rAd5/35 vector, further studies to compare with other rAd vectors may be needed. However, our results suggest that the rAd5/35 vector-based vaccine either alone or combined with DNA vaccine elicited a high frequency of viral-specific cellular T cell response that may well be key to controlling the acute and chronic phases of infection.

In conclusion, we have demonstrated that high doses of rAd5/35 vector-based vaccine afford protective immunity against SHIV in macaques. Since the rAd5/35 vector-based vaccine can bypass preexisting anti-Ad5 immunity, therAd5/35-based vaccine may offer considerable promise as an HIV vaccine.

Materials and methods

Animals

Fourteen adult cynomolgus macaques (*Macaca fascicularis*) were used in this study. The macaques were fed and cared for in accordance with the standard operating procedure approved by the Ministry of Education, Culture, Sports, Science and Technology of Japan. The study was performed in the P3 facility under guidelines established by the laboratory biosafety manual of World Health Organization (Someya et al., 2005).

Preparation of DNA and recombinant adenoviral vectors

A eukaryotic expression plasmid, pcDNA3.1 (−) (Invitrogen, Carlsbad, CA), was used as a backbone of the DNA vaccines that encode the SIVmac239 *gag* gene (rDNA-Gag) and HIV-1 89.6 *env* gp160 gene (rDNA-Env), and both DNA vaccines were constructed as previously described according to the standard protocol (Someya et al., 2004). The SIV and HIV DNAs for the DNA vaccines were not modified using humanized codon. No foreign gene encoding pcDNA 3.1 (−) was used as a control DNA vaccine (cDNA).

The E1 and E3 regions deleted recombinant Ad5/35 vectors that encoded the SIVmac239 *gag* gene (rAd5/35-Gag) and HIV-1 89.6 *env* gp160 gene (rAd5/35-Env) were constructed with an Ad generation kit (Avior Therapeutics, Inc., Seattle, WA) as previously described (Xin et al., 2005; Mizuguchi and Hayakawa, 2002). Briefly, SIV *gag* and HIV *env* PCR fragments driven by a CAG promoter were inserted into a shuttle plasmid, pLHSP (Avior Therapeutics, Inc.), before being transfected to human embryonic kidney (HEK293) cells. The recombinant vectors were purified by CsCl gradient centrifugation, and the total concentration of virus particles was calculated from the optical density at 260 nm (OD_{260}), using the formula 1 $OD_{260} = 1 \times 10^{12}$ virus particles/ml.

Immunizations and viral challenge

Four animals of the rDNA group (numbered M-1 through M-4) received three intramuscular injections of both 2.5 mg of rDNA-Gag and 2.5 mg of rDNA-Env at 8-week intervals (Weeks 0, 8 and 16), followed by two intradermal injections of control Ad5/35 expressing the gene LacZ (cAd5/35, 2×10^{11} particles of each) at 2-week intervals (Weeks 150 and 152). Four animals of the prime-boost group (numbered M-5 through M-8) received three injections of both 2.5 mg of rDNA-Gag and 2.5 mg of rDNA-Env, followed by two injections with both 10^{11} particles of rAd5/35-Gag and 10^{11} particles of rAd5/35-Env. Two animals of the rAd5/35 group (numbered M-9 and M-10) received three injections of 5 mg of cDNA, followed by two injections with both 10^{11} particles of rAd5/35-Gag and 10^{11} particles of rAd5/35-Env. The four control animals of the control group (numbered M-11 through M-14) received three injections of 5 mg of cDNA, followed by two injections with 2×10^{11} particles of cAd5/35 (Table 1). All animals received an intravenous challenge with twenty 50% tissue culture infectious doses ($TCID_{50}$) of highly pathogenic SHIV that originated from SHIV-89.6 (Someya et al., 2006; Shinohara et al., 1998, Lu et al., 1996; Reimann et al., 1996) 2 weeks after final immunization (at 154 weeks, Table 1).

Cellular immune response to SIV Gag and HIV Env

The cellular immune responses against SIV Gag and HIV Env were monitored by IFN-γ ELISPOT assay using SIVmac239 Gag peptide pools spanning the full length of the Gag protein and HIV-89.6 Env V3 peptides as previously described (Someya et al., 2005, 2006). Freshly isolated peripheral blood mononuclear cells were added to 96-well plates in triplicate at 2×10^5 cells/well and then incubated for 16 h with Gag peptide pools or V3 peptide. Individual IFN-γ spot-forming cells (SFC) were counted by using a KS ELISPOT compact system (Carl Zeiss, Jena, Germany). An SFC was defined as a large black spot with a fuzzy border (Mothe et al., 2002).

Antibody responses to SIV Gag and HIV Env

The humoral immune responses were determined by measuring anti-Gag- and anti-Env-specific IgG titers using ELISA as previously described (Someya et al., 2005, 2006). Ninety-six-well ELISA plates were coated with 1 μg/ml of SIV p27 Gag (Advanced Biotechnologies, Advanced Biotechnologies, Woburn, MA) or 5 μg/ml of SHIV 89.6P Env peptide (AIDS Research and Reference Program, National Institutes of Health, Rockville, MD). Heat-inactivated sera were serially diluted and then added to the ELISA plate. Anti-Gag- and-Env-V3-specific IgG bound to the antigens were detected with alkaline phosphatase-labeled goat anti-monkey IgG (EY Laboratories, Inc., San Mateo, CA) and *p*-nitrophenyl-phosphate disodium substrate (Invitrogen, Carlsbad, CA).

The SHIV-specific neutralization antibody assay was performed as previously described (Someya et al., 2005, 2006). In brief, 5 μg/ml of purified serum IgG was incubated with 100 $TCID_{50}$ of SHIV-C2/1 and then cultured in M8166 cells. The result was compared with cultures to which preimmune IgG had been added. Neutralization was expressed as the percent inhibition of SIV Gag production in the culture supernatant. The average results+6 SD of serum Ig from normal healthy monkeys were used as the cutoff for a positive titer (Someya et al., 2006).

Plasma viral RNA levels and $CD4^+$ T cell counts

SHIV RNA levels in plasma samples were determined by real-time PCR with a PRISM 7700 sequence detection system (Perkin-Elmer Applied Biosystems, Forest City, CA) as previously described (Someya et al., 2006; Sasaki et al., 2002). All RNA samples were amplified in duplicate. Data were expressed as RNA copies per milliliter.

$CD4^+$ T cell numbers were measured using a FACS Calibur flow cytometer system (Becton-Dickinson Bioscience, San Jose, CA) as previously described (Someya et al., 2006; Yoshino et al., 2000). Fifty microliters of whole blood specimens was stained

with anti-human CD3 (clone HIT3a, Becton-Dickinson), anti-human CD4 (clone SK3 Becton-Dickinson) and anti-human CD8 (clone SK1, Becton-Dickinson). CD3/CD4 effective T cell counts were analyzed using Cell Quest software (Becton-Dickinson).

Statistical analysis

Comparisons of test results among groups of animals were performed using the Kruskal–Wallis *H*-test followed by Student–Newman–Keuls correction.

Acknowledgments

We thank Dr. Nao Jounai of the Department of Molecular Biodefense Research, Yokohama City University, School of Medicine for his technical support.

References

Abbink, P., Lemckert, A.A., Ewald, B.A., Lynch, D.M., Denholtz, M., Smits, S., Holterman, L., Damen, I., Vogels, R., Thorner, A.R., O'Brien, K.L., Carville, A., Mansfield, K.G., Goudsmit, J., Havenga, M.J., Barouch, D.H., 2007. Comparative seroprevalence and immunogenicity of six rare serotype recombinant adenovirus vaccine vectors from subgroups B and D. J. Virol. 81, 4654–4663.

Amara, R.R., Villinger, F., Altman, J.D., Lydy, S.L., O'Neil, S.P., Staprans, S.I., Montefiori, D.C., Xu, Y., Herndon, J.G., Wyatt, L.S., Candido, M.A., Kozyr, N.L., Earl, P.L., Smith, J.M., Ma, H.L., Grimm, B.D., Hulsey, M.L., McClure, H.M., McNicholl, J.M., Moss, B., Robinson, H.L., 2001. Control of a mucosal challenge and prevention of AIDS by a multiprotein DNA/MVA vaccine. Science 292, 69–74.

Ami, Y., Izumi, Y., Matsuo, K., Someya, K., Kanekiyo, M., Horibata, S., Yoshino, N., Sakai, K., Shinohara, K., Yamazaki, S., Yamamoto, N., Honda, M., 2005. Prime-boost vaccination with recombinant Mycobacterium bovis Bacillus Calmette Guérin and a non-replicating vaccinia virus recombinant leads to long-lasting and effective immunity. J. Virol. 79, 12871–12879.

Barouch, D.H., Pau, M.G., Custers, J.H., Koudstaal, W., Kostense, S., Havenga, M.J., Truitt, D.M., Sumida, S.M., Kishko, M.G., Arthur, J.C., Korioth-Schmitz, B., Newberg, M.H., Gorgone, D.A., Lifton, M.A., Panicali, D.L., Nabel, G.J., Letvin, N.L., Goudsmit, J., 2004. Immunogenicity of recombinant adenovirus serotype 35 vaccine in the presence of pre-existing anti-Ad5 immunity. J. Immunol. 15, 6290–6297.

Barratt-Boyes, S.M., Soloff, A.C., Gao, W., Nwanegbo, E., Liu, X., Rajakumar, P.A., Brown, K.N., Robbins, P.D., Murphey-Corb, M., Day, R.D., Gambotto, A., 2006. Broad cellular immunity with robust memory responses to simian immunodeficiency virus following serial vaccination with adenovirus 5- and 35-based vectors. J. Gen. Virol. 87 (Pt. 1), 139–149.

Casimiro, D.R., Chen, L., Fu, T.M., Evans, R.K., Caulfield, M.J., Davies, M.E., Tang, A., Chen, M., Huang, L., Harris, V., Freed, D.C., Wilson, K.A., Dubey, S., Zhu, D.M., Nawrocki, D., Mach, H., Troutman, R., Isopi, L., Williams, D., Hurni, W., Xu, Z., Smith, J.G., Wang, S., Liu, X., Guan, L., Long, R., Trigona, W., Heidecker, G.J., Perry, H.C., Persaud, N., Toner, T.J., Su, Q., Liang, X., Youil, R., Chastain, M., Bett, A.J., Volkin, D.B., Emini, E.A., Shiver, J.W., 2003. Comparative immunogenicity in rhesus monkeys of DNA plasmid, recombinant vaccinia virus, and replication-defective adenovirus vectors expressing a human immunodeficiency virus type 1 *gag* gene. J. Virol. 77, 6305–6313.

Catanzaro, A.T., Koup, R.A., Roederer, M., Bailer, R.T., Enama, M.E., Moodie, Z., Gu, L., Martin, J.E., Novik, L., Chakrabarti, B.K., Butman, B.T., Gall, J.G.D., Richter King, C., Andrews, C.A., Sheets, R., Gomez, P.L., Mascola, J.R., Nabel, G.J., Graham, B.S., the Vaccine Research Center 006 Study Team, 2006. Phase 1 safety and immunogenicity evaluation of a multiclade HIV-1 candidate vaccine delivered by a replication-defective recombinant adenovirus vector. J. Infect. Dis. 194, 1638–1649.

De Jong, J.C., Wermenbol, A.G., Verweij-Uijterwaal, M.W., Slaterus, K.W., Wertheim-Van Dillen, P., Van Doornum, G.J., Khoo, S.H., Hierholzer, J.C., 1997. Adenoviruses from human immunodeficiency virus-infected individuals, including two strains that represent new candidate serotypes Ad50 and Ad51 of species B1 and D, respectively. J. Clin. Microbiol. 37, 3940–3945.

Eda, Y., Murakami, T., Ami, Y., Nakasone, T., Takizawa, M., Someya, K., Kaizu, M., Izumi, Y., Yoshino, N., Matsushita, S., Higuchi, H., Matsui, H., Shinohara, K., Takeuchi, H., Koyanagi, Y., Yamamoto, N., Honda, M., 2006. Anti-V3 humanized antibody KD-247 effectively suppresses ex vivo generation of human immunodeficiency virus type 1 and affords sterile protection of monkeys against a heterologous simian/human immunodeficiency virus infection. J. Virol. 80, 5563–5570.

Gaggar, A., Shayakhmetov, D.M., Lieber, A., 2003. CD46 is a cellular receptor for group B adenoviruses. Nat. Med. 9, 1408–1412.

Imler, J.L., 1995. Adenovirus vectors as recombinant viral vaccines. Vaccine 13, 1143–1151.

Kostense, S., Koudstaal, W., Sprangers, M., Weverling, G.J., Penders, G., Helmus, N., Vogels, R., Bakker, M., Berkhout, B., Havenga, M., Goudsmit, J., 2004. Adenovirus types 5 and 35 seroprevalence in AIDS risk groups supports type 35 as a vaccine vector. AIDS 18, 1213–1216.

Lemckert, A.A., Sumida, S.M., Holterman, L., Vogels, R., Truitt, D.M., Lynch, D.M., Nanda, A., Ewald, B.A., Gorgone, D.A., Lifton, M.A., Goudsmit, J., Havenga, M.J., Barouch, D.H., 2005. Immunogenicity of heterologous prime-boost regimens involving recombinant adenovirus serotype 11 (Ad11) and Ad35 vaccine vectors in the presence of anti-ad5 immunity. J Virol. 79, 9694–9701.

Letvin, N.L., Barouch, D.H., Montefiori, D.C., 2002. Prospect for vaccine protection against HIV-1 Infection and AIDS. Annu. Rev. Immunol. 20, 73–99.

Lu, Y., Salvato, M.S., Pauza, C.D., Li, J., Sodroski, J., Manson, K., Wyand, M., Letvin, N., Jenkins, S., Touzjian, N., Chutkowski, C., Kushner, N., LeFaile, M., Payne, L.G., Roberts, B., 1996. Utility of SHIV for testing HIV-1 vaccine candidates in macaques. J. Acquired Immune Defic. Syndr. Hum. Retrovirol. 12, 99–106.

Marttila, M., Persson, D., Gustafsson, D., Kathryn Liszewski, M.K., John, P., Atkinson, J.P., Wadell, G., Niklas Arnberg, N., 2005. CD46 is a cellular receptor for all species B adenoviruses except types 3 and 7. J. Virol. 79, 14429–14436.

Mascola, J.R., 2003. Defining the protective antibody response for HIV-1. Curr. Mol. Med. 3, 209–216.

Mascola, J.R., Sambor, A., Beaudry, K., Santra, S., Welcher, B., Louder, M.K., Vancott, T.C., Huang, Y., Chakrabarti, B.K., Kong, W.P., Yang, Z.Y., Xu, L., Montefiori, D.C., Nabel, G.J., Letvin, N.L., 2005. Neutralizing antibodies elicited by immunization of monkeys with DNA plasmids and recombinant adenoviral vectors expressing human immunodeficiency virus type 1 proteins. J. Virol. 79, 771–779.

Mellors, J.W., Rinaldo, C.R.Jr., Gupta, P., White, R.M., Todd, J.A., Kingsley, L.A., 1996. Prognosis in HIV-1 infection predicted by the quantity of virus in plasma. Science 272, 1167–1170.

Mellors, J.W., Munoz, A., Giorgi, J.V., Margolick, J.B., Tassoni, C.J., Gupta, P., Kingsley, L.A., Todd, J.A., Saah, A.J., Detels, R., Phair, J.P., Rinaldo Jr., C.R., 1997. Plasma viral load and $CD4^+$ lymphocytes as prognostic markers of HIV-1 infection. Ann. Intern. Med. 126, 946–954.

Mizuguchi, H., Hayakawa, T., 2002. Adenovirus vectors containing chimeric type 5 and type 35 fiber proteins exhibit altered and expanded tropism and increase the size limit of foreign genes. Gene 285, 69–77.

Mothe, B.R., Horton, H., Carter, D.K., Allen, T.M., Liebl, M.E., Skinner, P., Vogel, T.U., Fuenger, S., Vielhuber, K., Rehrauer, W., Wilson, N., Franchini, G., Altman, J.D., Haase, A., Picker, L.J., Allison, D.B., Watkins, D.I., 2002. Dominance of CD8 responses specific for epitopes bound by a single major histocompatibility complex class I molecule during the acute phase of viral infection. J. Virol. 76, 875–884.

Musey, L., Hughes, J., Schacker, T., Shea, T., Corey, L., McElrath, M.L., 1997. Cytotoxic T-cell responses, viral load, and disease progression in early human immunodeficiency virus type 1 infection. N. Engl. J. Med. 30, 1267–1274.

Ophorst, O.J., Kostense, S., Goudsmit, J., De Swart, R.L., Verhaagh, S., Zakhartchouk, A., Van Meijer, M., Sprangers, M., Van Amerongen, G., Yuksel, S., Osterhaus, A.D., Havenga, M.J., 2004. An adenoviral type 5 vector carrying a type 35 fiber as a vaccine vehicle: DC targeting, cross neutralization, and immunogenicity. Vaccine 22, 3035–3044.

Patke, D.S., Langan, S.J., Carruth, L.M., Keating, S.M., Sabundayo, B.P., Margolick, J.B., Quinn, T.C., Bollinger, R.C., 2002. Association of Gag-specific T lymphocyte responses during the early phase of human immunodeficiency virus type 1 infection and lower virus load set point. J. Infect. Dis. 186, 1177–1180.

Rea, D., Havenga, M.J., van Den Assem, M., Sutmuller, R.P., Lemckert, A., Hoeben, R.C., Bout, A., Melief, C.J., Offringa, R., 2001. Highly efficient transduction of human monocyte-derived dendritic cells with subgroup B fiber-modified adenovirus vectors enhances transgene-encoded antigen presentation to cytotoxic T cells. J. Immunol. 166, 5236–5244.

Reimann, K.A., Li, J.T., Voss, G., Lekutis, C., Tenner-Racz, K., Racz, P., Lin, W., Montefiori, D.C., Lee-Parritz, D.E., Lu, Y., Collman, R.G., Sodroski, J., Letvin, N.L., 1996. An *env* gene derived from a primary human immunodeficiency virus type 1 isolate confers high in vivo replicative capacity to a chimeric simian/human immunodeficiency virus in rhesus monkeys. J. Virol. 70, 3198–3206.

Roberts, D.M., Nanda, A., Havenga, M.J., Abbink, P., Lynch, D.M., Ewald, B.A., Liu, J., Thorner, A.R., Swanson, P.E., Gorgone, D.A., Lifton, M.A., Lemckert, A.A., Holterman, L., Chen, B., Dilraj, A., Carville, A., Mansfield, K.G., Goudsmit, J., Barouch, D.H., 2006. Hexon-chimaeric adenovirus serotype 5 vectors circumvent pre-existing anti-vector immunity. Nature 441, 239–243.

Sasaki, Y., Ami, Y., Nakasone, T., Shinohara, K., Takahashi, E., Ando, S., Someya, K., Suzaki, Y., Honda, M., 2002. Induction of CD95 ligand expression on T lymphocytes and B lymphocytes and its contribution to apoptosis of CD95-upregulated $CD4^+$ T lymphocytes in macaques by infection with a pathogenic simian/human immunodeficiency virus. Clin. Exp. Immunol. 122, 381–389.

Segerman, A., Mei, Y.F., Wadell, G., 2000. Adenovirus types 11p and 35p show high binding efficiencies for committed hematopoietic cell lines and are infective to these cell lines. J. Virol. 74, 1457–1467.

Shayakhmetov, D.M., Papayannopoulou, T., Stamatoyannopoulos, G., Lieber, A., 2000. Efficient gene transfer into human CD34 (+) cells by a retargeted adenovirus vector. J. Virol. 74, 2567–2583.

Shinohara, K., Sakai, K., Ando, S., Ami, Y., Yoshino, N., Takahashi, E., Someya, K., Suzaki, Y., Nakasone, T., Sasaki, Y., Kaizu, M., Lu, Y., Honda, M., 1998. A highly pathogenic simian/human immunodeficiency virus with genetic changes in cynomolgus monkeys. J. Gen. Virol. 80 (Pt. 5), 1231–1240.

Shiver, J.W., Fu, T.M., Chen, L., Casimiro, D.R., Davies, M.E., Evans, R.K., Zhang, Z.Q., Simon, A.J., Trigona, W.L., Dubey, S.A., Huang, L., Harris, V.A., Long, R.S., Liang, X., Handt, L., Schleif, W.A., Zhu, L., Freed, D.C., Persaud, N.V., Guan, L., Punt, K.S., Tang, A., Chen, M., Wilson, K.A., Collins, K.B., Heidecker, G.J., Fernandez, V.R., Perry, H.C., Joyce, J.G., Grimm, K.M., Cook, J.C., Keller, P.M., Kresock, D.S., Mach, H., Troutman, R.D., Isopi, L.A., Williams, D.M., Xu, Z., Bohannon, K.E., Volkin, D.B., Montefiori, D.C., Miura, A., Krivulka, G.R., Lifton, M.A., Kuroda, M.J., Schmitz, J.E., Letvin, N.L., Caulfield, M.J., Bett, A.J., Youil, R., Kaslow, D.C., Emini, E.A., 2002. Replication-incompetent adenoviral vaccine vector elicits effective anti-immunodeficiency-virus immunity. Nature 415, 331–335.

Someya, K., Xin, K.Q., Matsuo, K., Okuda, K., Yamamoto, N., Honda, M., 2004. A consecutive priming-boosting vaccination of mice with simian immunodeficiency virus (SIV) gag/pol DNA and recombinant vaccinia virus strain DIs elicits effective anti-SIV immunity. J. Virol. 78, 9842–9853.

Someya, K., Cecilia, D., Ami, Y., Nakasone, T., Matsuo, K., Burda, S., Yamamoto, H., Yoshino, N., Kaizu, M., Ando, S., Okuda, K., Zolla-Pazner, S., Yamazaki, S., Yamamoto, N., Honda, M., 2005. Vaccination of rhesus macaques with recombinant Mycobacterium bovis bacillus Calmette–Guérin Env V3 elicits neutralizing antibody-mediated protection against simian–human immunodeficiency virus with a homologous but not a heterologous V3 motif. J. Virol. 79, 1452–1462.

Someya, K., Ami, Y., Nakasone, T., Izumi, Y., Matsuo, K., Horibata, S., Xin, K.Q., Yamamoto, H., Okuda, K., Yamamoto, N., Honda, M., 2006. Induction of effective cellular and humoral immune responses by a prime-boost vaccine encoded with simian immunodeficiency virus gag/pol. J. Immunol. 176, 1784–1795.

Vogels, R., Zuijdgeest, D., van Rijnsoever, R., Hartkoorn, E., Damen, I., de Bethune, M.P., Kostense, S., Penders, G., Helmus, N., Koudstaal, W., Cecchini, M., Wetterwald, A., Sprangers, M., Lemckert, A., Ophorst, O., Koel, B., van Meerendonk, M., Quax, P., Panitti, L., Grimbergen, J., Bout, A., Goudsmit, J., Havenga, M., 2003. Replication-deficient human adenovirus type 35 vectors for gene transfer and vaccination: efficient human cell infection and bypass of preexisting adenovirus immunity. J. Virol. 77, 8263–8271.

Xin, K.Q., Jounai, N., Someya, K., Honma, K., Mizuguchi, H., Naganawa, S., Kitamura, K., Hayakawa, T., Saha, S., Takeshita, F., Okuda, K., Honda, M., Klinman, D.M., Okuda, K., 2005. Prime-boost vaccination with plasmid DNA and a chimeric adenovirus type 5 vector with type 35 fiber induces protective immunity against HIV. Gene Ther. 12, 1769–1777.

Xin, K.Q., Sekimoto, Y., Takahashi, T., Mizuguchi, H., Ichino, M., Yoshida, A., Okuda, K., 2007. Chimeric adenovirus 5/35 vector containing the clade C HIV *gag* gene induces a cross-reactive immune response against HIV. Vaccine 25, 3809–3815.

Yoshino, N., Ami, Y., Terao, K., Tashiro, F., Honda, M., 2000. Upgrading of flow cytometric analysis for absolute counts, cytokines and other antigenic molecules of cynomolgus monkeys (*Macaca fascicularis*) by using anti-human cross-reactive antibodies. Exp. Anim. 49, 97–110.